

PVT MEASUREMENTS ON FLUOROFORM: SECOND AND THIRD  
VIRIAL COEFFICIENTS FROM 200°C TO 350°C AND  
COMPRESSIBILITY FACTORS TO 150 ATMOSPHERES

---

A DISSERTATION  
PRESENTED TO  
THE FACULTY OF THE GRADUATE SCHOOL  
UNIVERSITY OF MISSOURI

---

IN PARTIAL FULFILLMENT  
OF THE REQUIREMENTS FOR THE DEGREE  
DOCTOR OF PHILOSOPHY

---

BY  
WEN-SHOU LIOU

JUNE 1974

TRUMAN S. STORVICK DISSERTATION SUPERVISOR

PVT MEASUREMENTS ON FLUOROFORM: SECOND AND THIRD  
VIRIAL COEFFICIENTS FROM 200°C TO 350°C AND  
COMPRESSIBILITY FACTORS TO 150 ATMOSPHERES

Wen-Shou Liou

Truman S. Storvick Dissertation Supervisor

ABSTRACT

The Burnett method was employed to study the volumetric behavior of fluoroform gas from 200 to 350°C at pressure up to 150 atmospheres. An estimate of the assignable measurement errors indicate the data should be accurate to 5 part in 10,000. A nonlinear regression analysis method was used to evaluate the second and the third virial coefficients of fluoroform gas. This data analysis method considers both the dependent and the independent variables are subject to error and eliminates the need for prior knowledge of the run constant and the apparatus constant to evaluate the second and the third virial coefficients of the gas. The parameters of Benedict-Webb-Rubin equation of state were evaluated by using the experimental Burnett p-v-T measurements. The Benedict-Webb-Rubin equation of state represents the data within the experimental error of the measurements.

## VITA

Liou Wen-Shou was born in KiangSi, China, on April 15, 1940, the second son of Gen. and Mrs. C. H. Liou, Ret.. He received his elementary education in SanTong, KiangSo, Taiwan, China. In 1958, he received his high school diploma from The High School of Taiwan Normal University, Taipei, Taiwan, China. In the same year, he enrolled in Chungyuan Christian College of Science and Engineering, ChungLi, Taiwan, China. He graduated with the degree of Bachelor of Science in Chemical Engineering in June, 1963.

He was commissioned second Lieutenant in the Republic of China Military Police in September, 1962. He served in The Taiwan Garrison Headquarters as a special inspector until August, 1963.

The author entered the graduate school of South Dakota School of Mines and Technology, Rapid City, South Dakota, September, 1963. He graduated with the degree of Master of Science in Chemical Engineering in June, 1966. The title of his master thesis was "Vapor-liquid Equilibrium at Sub-atmospheric Pressure of the 1-Butanol and Benzene System," prepared under the direction of Dr. R. L. Sandvig.

After one year of industrial experience, the author enrolled in graduate school at the University of Missouri, Columbia, Missouri.

He is married to the former Daisy Chen-Shew Hsia of Nanking, China. They have one living son, Albert Ta-Chen.

## ACKNOWLEDGEMENTS

The author wishes to express his sincere appreciation to Dr. Truman S. Storvick for his invaluable patience, guidance, and assistance during the course of this project. Thanks are also due other members of the university staff, especially Mr. Joe Twenter and Mr. Bill Carter for their willing to help in any situation when asked.

Dr. H. I. Britt and Dr. R. H. Luecke must be remembered because of the excellent computer program of nonlinear regression analysis for reduction Burnett p-v-T measurements to virial coefficients was used in this work.

Dr. R. F. Hein of E.I. Du Pont De Nemours & Company for his generous donation of highly purified fluoroform gas.

The financial support of the National Science Foundation was gratefully received.

Finally, the author wishes to thank his parents and his wife for their countless continuous encouragement, understanding, and patience in the preparation of this work.

## TABLE OF CONTENTS

CHAPTER	PAGE
I. INTRODUCTION . . . . .	1
II. METHOD OF REDUCTION OF BURNETT EXPERIMENTAL DATA TO COMPRESSIBILITY FACTORS AND VIRIAL COEFFICIENTS . . . . .	6
A. STATISTICAL ANALYSIS OF THE BURNETT MEASUREMENTS TO OBTAIN VIRIAL COEFFICIENTS . . . . .	7
B. REGRESSION ANALYSIS TO OBTAIN CONSTANTS OF BENEDICT-WEBB-RUBIN EQUATION OF STATE . . . . .	18
III. EXPERIMENTAL APPARATUS AND PROCEDURE . . . . .	20
A. EXPERIMENTAL APPARATUS . . . . .	20
B. EXPERIMENTAL PROCEDURE . . . . .	29
IV. RESULTS AND DISCUSSIONS . . . . .	33
A. CALIBRATION OF BURNETT CELL WITH HELIUM . . . . .	33
B. FLUOROFORM DATA . . . . .	34
C. ERROR ANALYSIS . . . . .	35
V. CONCLUSIONS AND RECOMMENDATIONS . . . . .	38
A. CONCLUSIONS . . . . .	38
B. RECOMMENDATIONS . . . . .	39
FIGURES AND TABLES . . . . .	42
LIST OF SYMBOLS USED IN FIGURES . . . . .	44
BIBLIOGRAPHY . . . . .	67

CHAPTER	PAGE
APPENDICES . . . . .	72
A. METHOD OF NONLINEAR REGRESSION . . . . .	73
B. DESCRIPTION OF THE MEASURING INSTRUMENTS . . . . .	84
C. CORRECTIONS FOR PRESSURE MEASUREMENTS . . . . .	98
D. COMPUTER PROGRAM USED TO EVALUATE THE SECOND AND THE THIRD VIRIAL COEFFICIENTS FROM BURNETT P-V-T MEASUREMENTS . . . . .	.106
E. ORIGINAL DATA . . . . .	.122

## LIST OF FIGURES

FIGURE	PAGE
1. Schematic Diagram of Pressure Measurement and Charging System . . . . .	42
2. Schematic Diagram of Thermal and Vacuum System .	43
3. The Burnett Cell . . . . .	48
4. The Expansion Valve . . . . .	49
5. The Experimental Apparatus . . . . .	50
6. The Pressure Measurement Devices . . . . .	51
7. The Contents of the Constant Temperature Bath .	52
8. The Temperature Control and Measurement Devices.	53
9. Temperature versus Second Virial Coefficients of Fluoroform . . . . .	54
10. Temperature versus Third Virial Coefficients of Fluoroform . . . . .	55

## LIST OF TABLES

TABLE	PAGE
1. Numerical Values of the Constants in Benedict-Webb-Rubin Equation of State for Fluoroform (English Units) . . . . .	56
2. Numerical Values of the Constants in Benedict-Webb-Rubin Equation of State for Fluoroform (Metric Units) . . . . .	57
3. Helium Measurements: Second and Third Virial Coefficients, Apparatus Constants, and the Standard Error of Estimate by Nonlinear Analysis . . . . .	58
4. Average Values of the Second and the Third Virial Coefficients, Apparatus Constants from the Helium Measurements, and the Standard Error of Estimate by Nonlinear Analysis . . . . .	59
5. Comparison of Second Virial Coefficients of Helium . . . . .	60
6. Fluoroform Measurements: Second and Third Virial Coefficients, Apparatus Constants, and the Standard Error of Estimate by Nonlinear Analysis . . . . .	61



TABLE	PAGE
7. Average Values of the Second and the Third Virial Coefficients, Apparatus Constants from the Fluoroform Measurements, and the Standard Error of Estimate by Nonlinear Analysis . . . .	62
8. Experimental Values of Run Constant and Compressibility Factors for Fluoroform . . . .	63
E-1. Original Data . . . . .	.122
E-2. Dead Weight Gauge Constants and Weight Calibrations . . . . .	.139

## CHAPTER I

### INTRODUCTION

The search for new physical property information is as endless as the search for new chemical systems and new conditions for processing and application. Demands for accurate values of bulk properties are consistently made. Although statistical mechanics can be used to describe the configurational properties of the fluids, yet it requires information about the intermolecular forces. One primary source of information about molecular forces is the experimental measurements of physical properties.

The best known application of configurational statistical mechanics is provided by the virial equation of state which express  $Z$ , the compressibility factor of gas, as a power series in density  $\rho$  in

$$Z = \frac{pv}{RT} = 1 + B\rho + C\rho^2 + \dots \quad (\text{I-1})$$

For a gas at constant composition, the virial coefficients  $B, C, \dots$  are function only of temperature (43).

The statistical mechanical derivation of equation (I-1) is discussed in several texts (12,28,37). From

statistical mechanics, one obtains the equation of state

$$p = kT \left( \frac{\partial \ln Z_N}{\partial v} \right)_T \quad (\text{I-2})$$

where  $Z_N$  is the partition function for the gas.

From this we see that the configurational part of the partition function  $Z_N$ , must be obtained to get the equation of state. If we write the system Hamiltonian as the sum of the kinetic energy of each particle  $p_i^2/2m_i$  plus a potential energy term that depends on the system configuration  $\Phi(\underline{r}^N)$ ,

$$H(\underline{r}^N, \underline{p}^N) = \sum_{i=1}^N \frac{p_i^2}{2m_i} + \Phi(\underline{r}^N) \quad (\text{I-3})$$

then we get a density expansion for  $pv/kT$  again that is the same form as the virial expansion equation (I-1). Further, the coefficient of the  $\rho$  term from this procedure leads to a configuration integral that involves only molecules interacting in pairs. The coefficient of  $\rho^2$  depends upon interactions between three particles, etc. In order to do this expansion one must assume that  $\Phi(\underline{r}^N)$  can be split up into a sum of contributions for pairs, three particles, etc. The procedure is complicated and was first treated in detail by Meyer (39) in 1937.

One can also get the virial equation of state from the virial theorem of mechanics (37). The virial theorem

states that the average kinetic energy of total system is given by

$$\bar{K} = \frac{1}{2} \sum_i v_i^2 m_i = -\frac{1}{2} \sum_i \overline{\underline{r}_i \cdot \underline{F}_i} \quad (\text{I-4})$$

where  $\underline{F}$  is the force acting on the particle. This leads to an equation in terms of the radical pair distribution function. This procedure is usually applied to liquids rather than gases. It is more cumbersome to use because one must now expand the radical pair distribution function in a power series in density.

It is important to maintain a clear distinction between experimental coefficients (coefficients obtained from equation (I-1)) and mathematical relationships between pair potentials and the density expansions from statistical mechanics.

Knowledge of experimental second virial coefficients over a wide range of temperature, preferable from the triple point temperature to the dissociation temperature, may be used to evaluate the parameters in an intermolecular potential function and to calculate the thermodynamic and transport properties for that substances (29,57).

Knowledge of experimental third virial coefficients provides information about molecular three particle interactions. The unsolved three-particle dynamics problem make it necessary to consider the intermolecular forces as pairwise additive. The magnitude of the deviations from the

pair-wise additive model are not well established. Using the pair-wise interaction model developed from experimental second virial coefficients and the transport properties, the proposed non-additive corrections can be examined by comparing them with experimental third virial coefficients (13, 14, 37, 38, 54).

Little is known about fourth and higher virial coefficients although several theoretical studies of higher virial coefficients have been reported (2, 47).

The purpose of this work is to show how the virial coefficients, both the second and the third, can be experimentally determined from the Burnett (11) p-v-T measurements. A special nonlinear regression analysis method was used to obtain the experimental virial coefficients from the Burnett p-v-T measurements. This new data analysis method eliminates the need for prior knowledge of the instrument run constant and the apparatus constant to obtain the gas compressibility factors and for evaluating the second and the third virial coefficients of the sample gas. The parameters for the Benedict-Webb-Rubin equation of state are evaluated by using the experimental p-v-T data. The compressibility factors given by the BWR equation are in excellent agreement with the original data.

The Burnett method of measuring gas p-v-T behavior was introduced in 1936. Since then the procedure has been used by many investigators (1, 4, 5, 8, 17, 20, 23, 24, 25, 26, 32, 34, 36, 41, 42, 44, 45, 48, 49, 50, 51, 52, 53, 55, 56, 60, 61, 62, 63, 65, 67, 69)

over a wide range of temperatures and pressures to determine gas compressibility factors and virial coefficients. The main advantage of using the Burnett apparatus is that neither the volume of the apparatus nor the mass of the experimental gas need to be measured. Only the isothermal pressure measurements are required and these temperature, and pressures can be measured with high precision and accuracy. Based on these advantages the Burnett apparatus was selected for this investigation.

Fluoroform was chosen for this investigation because it is a simple polar molecule (dipole moment = 1.65 Debyes (64)). It is available in a very pure state (purity = 99.9899%min.). There are essentially no p-v-T measurement on fluoroform over 200°C and the data should be generally useful.

The second chapter describes the method for reducing the Burnett data to compressibility factors and to virial coefficients. The experimental apparatus and the procedure are described next followed by the results, discussion and conclusion sections. Recommendations are made for future work and the Appendixes contain descriptions of the instruments, and measurements, details of computations and the original experimental data.

## CHAPTER II

METHOD OF REDUCTION OF BURNETT EXPERIMENTAL DATA TO  
OBTAIN COMPRESSIBILITY FACTORS AND VIRIAL COEFFICIENTS

The Burnett p-v-T method (11) is based on an apparatus made of two cells of unspecified volume and connected by an expansion valve. The cells and the expansion valve are immersed in a constant temperature bath. To start a run, one cell is filled with test gas to some initial pressure and the other cell is evacuated. When thermal equilibrium is restored, the temperature and the cell pressure are recorded. The expansion valve is opened and when thermal equilibrium is restored the expansion valve is closed the cell temperature and pressure are again recorded. The second cell is evacuated and the process repeated to make another expansion. This procedure is continued until the pressure is too low for accurate pressure measurements. The sequence of isothermal pressure measurements constitutes a run. The process is then repeated with a different starting pressure a sufficient number of times to establish the isotherm.

A. Statistical Analysis of the Burnett Measurements to Obtain Virial Coefficients

The Burnett method can be analyzed using the compressibility factor equation of state. At a selected isotherm temperature  $T$ ,  $n_0$  moles of gas are charged into the first cell  $C_I$ . The pressure  $p_0$  is

$$p_0 C_I = n_0 Z_0 RT \quad (\text{II-1})$$

where  $R$  is the universal gas constant and  $Z_0$  is the compressibility factor of gas at initial pressure  $p_0$  and temperature  $T$ .

The change in volume of the Burnett cell  $C_I$  due to the internal pressure  $p_0$  can be expressed as,

$$\frac{\delta C_I}{(C_I)_0} = \alpha p_0 \quad (\text{II-2})$$

with  $\delta C_I = C_I - (C_I)_0$ . Volume  $(C_I)_0$  is the volume of the Burnett cell  $C_I$  at some arbitrary reference condition, which is taken as the isothermal volume at zero pressure. The pressure distortion coefficient  $\alpha$  for the cell has been shown to be (7),



$$\alpha = \frac{3(1 - 2\sigma)R_r^2 + 2(1 + \sigma)R_j^2}{E \times (R_j^2 - R_r^2)} \quad (\text{II-3})$$

where

$\sigma$  = Poisson's ratio

$E$  = Young's modulus

$R_r$  = radius to internal wall of the cell

$R_j$  = radius to external wall of the cell

Equation (II-2) can be rewritten as,

$$C_I = (C_I)_o (1 + \alpha p_o) \quad (\text{II-4})$$

After expansion into the preevacuated cell  $C_{II}$  the pressure  $p_o$  will be reduced to  $p_1$  due to the volume increase. At isothermal conditions,

$$p_1(C_I + C_{II}) = n_o Z_1 RT \quad (\text{II-5})$$

The change in volume of the Burnett cell  $(C_I + C_{II})$  due to the internal pressure change to  $p_1$  can be expressed as,

$$(C_I + C_{II}) = (C_I + C_{II})_o (1 + \alpha p_1) \quad (\text{II-6})$$

Dividing equation (II-5) by equation (II-1),

$$\frac{p_1}{p_0} N_1 = \frac{z_1}{z_0} \quad (\text{II-7})$$

where

$$N_1 = \left( \frac{C_I + C_{II}}{C_I} \right)_1 \quad (\text{II-8})$$

Substituting equation (II-4), (II-6) into equation (II-8),

$$N_1 = \left( \frac{C_I + C_{II}}{C_I} \right)_0 \left( \frac{1 + \alpha p_1}{1 + \alpha p_0} \right) \quad (\text{II-9})$$

or

$$N_1 = N_0 \left( \frac{1 + \alpha p_1}{1 + \alpha p_0} \right) \quad (\text{II-10})$$

Before the  $r^{\text{th}}$  expansion,

$$p_{r-1} C_I = n_{r-1} z_{r-1}^{RT} \quad (\text{II-11})$$

After the  $r^{\text{th}}$  expansion,

$$p_r (C_I + C_{II}) = n_{r-1} z_r^{RT} \quad (\text{II-12})$$

Dividing equation (II-12) by equation (II-11),

$$\frac{p_r}{p_{r-1}} N_r = \frac{Z_r}{Z_{r-1}} \quad (\text{II-13})$$

where

$$\begin{aligned} N_r &= \left( \frac{C_I + C_{II}}{C_I} \right)_r \\ &= \left( \frac{C_I + C_{II}}{C_I} \right)_0 \left( \frac{1 + \alpha p_r}{1 + \alpha p_{r-1}} \right) \\ &= N_0 \left( \frac{1 + \alpha p_r}{1 + \alpha p_{r-1}} \right) \end{aligned} \quad (\text{II-14})$$

Applying equation (II-13) and equation (II-14) to the first, second, ...  $r^{\text{th}}$  expansion and combining, the results are,

$$p_r \prod_{i=1}^r N(p_i, p_{i-1}) = (p_0/Z_0) Z_r \quad (\text{II-15})$$

Assuming at the low-pressure limit that the compressibility factor approaches unity, equation (II-15) becomes,

$$\lim_{p_r \rightarrow 0} p_r \prod_{i=1}^r N(p_i, p_{i-1}) = p_0/Z_0 \quad (\text{II-16})$$

One way to evaluate the run constant,  $p_0/Z_0$ , is to plot the  $p_r \pi N(p_i, p_{i-1})$  versus  $p_r$  and extrapolate to  $p_r = 0$ . In this work, the run constant for each series of expansions was calculated by substituting the apparatus constant,  $N$ , and the low-pressure range expansion pressure measurements into equation (II-16). The experimental compressibility factors for each expansion in a run were then obtained by using the run constant,  $(p_0/Z_0)$ , the apparatus constant,  $N$ , and the equation (II-15).

The compressibility factor  $Z$  can also be expressed by an infinite power series in pressure,

$$Z_{r-1} = 1 + \sum_{i=1}^{\infty} b_i p_{r-1}^i \quad (\text{II-17})$$

$$Z_r = 1 + \sum_{i=1}^{\infty} b_i p_r^i \quad (\text{II-18})$$

where  $b_i$  is the  $i^{\text{th}}$  coefficient in the pressure series. These expansion coefficients are related to the density virial coefficients (43) given in equation (I-1) by the following expressions (18,19,46),

$$\begin{aligned} B &= RTb_1 \\ C &= (RT)^2 (b_2 + b_1^2) \end{aligned} \quad (\text{II-19})$$

where  $B$ ,  $C$ , are the second and third virial coefficients, respectively.

Substituting  $Z_{r-1}$ ,  $Z_r$  into equation (II-13) for a run with  $S$  expansions, a residual function  $F_r(p,b)$  is obtained.

$$F_r(p,b) = p_{r-1}p_r \sum_{i=1}^{\infty} b_i (p_r^{i-1} - N_r p_{r-1}^{i-1}) \\ + p_{r-1} - N_r p_r \quad ; r = 1 \dots S \quad (\text{II-20})$$

Equation (II-20) will be zero when the pressures are known with absolute accuracy and equation (II-17) exactly represents  $Z_{r-1}$ . It will usually be nonzero because the pressure measurements are subject to experimental error and the compressibility factors expressed as infinite series in pressure must be truncated to a finite number of terms. Thus in terms of actual variables, equation (II-20) becomes,

$$F_r(p',b') = p'_{r-1}p'_r \sum_{i=1}^k b'_i (p_r'^{(i-1)} - N_r p'_{r-1}{}^{(i-1)}) \\ + p'_{r-1} - N_r p'_r \approx 0 \quad ; r = 1 \dots S \quad (\text{II-21})$$

where the primes indicate experimental measured or observed values. J.M.H. Levelt-Sengers (35) suggested a nonlinear regression method outlined in Appendix A which can be used to obtain the "best fit" of the coefficients in the pressure series from experimental measurements of the Burnett pressure sequences. Equation (II-21) is linearized by truncating its Taylor's expansion around the pressure and the  $b_i$  values in

equation (II-20) after the first derivatives. The results written in matrix form are,

$$\underline{F}(p', b') = \underline{F}(p, b) + \underline{F}_p \Delta p + \underline{F}_b \Delta b \quad (\text{II-22})$$

where  $\underline{F}$  is the S-vector,

$$\underline{F} = \begin{vmatrix} F_1 \\ \cdot \\ \cdot \\ \cdot \\ F_S \end{vmatrix} \quad (\text{II-23})$$

$\underline{F}_p^T$  is a (S, S+1) Jacobian matrix of F with respect to p,

$$\underline{F}_p^T = \begin{vmatrix} \frac{\partial F_1}{\partial p_0} & 0 & 0 & 0 & 0 \\ \frac{\partial F_1}{\partial p_1} & \frac{\partial F_2}{\partial p_1} & 0 & 0 & 0 \\ 0 & \frac{\partial F_2}{\partial p_2} & \cdot & 0 & 0 \\ 0 & 0 & \cdot & \cdot & 0 \\ 0 & 0 & 0 & \cdot & \frac{\partial F_S}{\partial p_{S-1}} \\ 0 & 0 & 0 & 0 & \frac{\partial F_S}{\partial p_S} \end{vmatrix} \quad (\text{II-24})$$

$\Delta \underline{p}$  is the  $(S+1)$ -vector,

$$\Delta \underline{p} = \begin{vmatrix} \Delta p_1 \\ \cdot \\ \cdot \\ \cdot \\ \Delta p_{S+1} \end{vmatrix} \quad (\text{II-25})$$

where

$$\Delta p_r = p_r' - p_r \quad ; \quad r = 1 \dots S \quad (\text{II-26})$$

$\underline{F}_b$  is a  $(S,k)$  Jacobian matrix of  $F$  with respect to  $b_i$ ,

$$\underline{F}_b = \begin{vmatrix} -\frac{\partial F_1}{\partial b_1} & \cdot & \cdot & \cdot & -\frac{\partial F_1}{\partial b_k} \\ \cdot & \cdot & \cdot & \cdot & \cdot \\ \cdot & \cdot & \cdot & \cdot & \cdot \\ \cdot & \cdot & \cdot & \cdot & \cdot \\ -\frac{\partial F_S}{\partial b_1} & \cdot & \cdot & \cdot & -\frac{\partial F_S}{\partial b_k} \end{vmatrix} \quad (\text{II-27})$$

and  $\Delta \underline{b}$  is the  $k$ -vector,

$$\Delta \underline{b} = \begin{vmatrix} \Delta b_1 \\ \cdot \\ \cdot \\ \cdot \\ \Delta b_k \end{vmatrix} \quad (\text{II-28})$$

with

$$\Delta b_i = b'_i - b_i \quad ; \quad i = 1 \dots k \quad (\text{II-29})$$

The elements of the Jacobian matrices are obtained from equation (II-21) by differentiating with respect to  $p_{r-1}$ ,  $p_r$ ,  $b_i$ , respectively, and dropping the primes to simplify the notation.

$$\begin{aligned} \frac{\partial F_r}{\partial p_{r-1}} &= 1 + \sum_{i=1}^k b_i p_r^i - N_r p_r \sum_{i=1}^k i b_i p_{r-1}^{i-1} + p_r N_r \\ &\quad \left( \frac{\alpha}{1 + \alpha p_{r-1}} \right) \left( 1 + \sum_{i=1}^k b_i p_{r-1}^i \right) \quad ; \\ &\quad r = 1 \dots S \end{aligned} \quad (\text{II-30})$$

$$\begin{aligned} \frac{\partial F_r}{\partial p_r} &= p_{r-1} \sum_{i=1}^k i b_i p_r^{i-1} - N_r \left( 1 + \sum_{i=1}^k b_i p_{r-1}^i \right) \\ &\quad - N_0 \left( \frac{\alpha p_r}{1 + \alpha p_{r-1}} \right) \left( 1 + \sum_{i=1}^k b_i p_{r-1}^i \right) \quad ; \\ &\quad r = 1 \dots S \end{aligned} \quad (\text{II-31})$$

$$\begin{aligned} \frac{\partial F_r}{\partial b_i} &= p_{r-1} p_r (p_r^{i-1} - N_r p_{r-1}^{i-1}) \quad ; \\ &\quad i = 1 \dots k \quad ; \quad r = 1 \dots S \end{aligned} \quad (\text{II-32})$$



Statistical weighting factors are assigned to the measured values by assuming the precision of the pressure measurements is constant, that the pressure measurements are uncorrelated and of unequal variance. The weighting matrix then becomes,

$$\underline{\underline{A}} = \begin{vmatrix} 1/w_1 & 0 & 0 & 0 & 0 \\ 0 & . & 0 & 0 & 0 \\ 0 & 0 & . & 0 & 0 \\ 0 & 0 & 0 & . & 0 \\ 0 & 0 & 0 & 0 & 1/w_{S+1} \end{vmatrix} \quad (\text{II-33})$$

The weighting factor  $w_i$  ( $i = 1 \dots S$ ) may be assigned a priori as proportional to  $p_i^2$  ( $i = 1 \dots S$ ). The functional form of this weighting factor is unknown and Blancett, Hall and Canfield (4) have shown that when arbitrary form  $w_i = (p_i + a)^2$  ( $i = 1 \dots S$ ) is used, a minimum variance is obtained when  $a = 3$ . This form was adopted without attempting to adjust the value of  $a$  with the experimental data.

When there are additional runs, each with  $S_1, S_2, \dots$  expansions, the  $\underline{\underline{F}}_p$  is a matrix of  $S_1 + 1 + S_2 + 1 + \dots$  rows by  $S_1 + S_2 + \dots$  columns,  $\underline{\underline{F}}_b$  is a matrix of  $S_1 + S_2 + \dots$  rows and  $k$  columns. The  $\underline{\underline{A}}$  matrix for several sets of consecutive uncorrelated pressure measurements can be formed by joining the  $\underline{\underline{A}}$  matrices of the individual sets of runs along the diagonal in the same order as for  $\underline{\underline{F}}_p$  and  $\underline{\underline{F}}_b$ .

An  $\underline{\underline{L}}$  matrix is then formed,

$$\underline{\underline{L}} = \underline{\underline{F}}_p^T \underline{\underline{A}} \underline{\underline{F}}_p \quad (\text{II-34})$$

With all of the matrices defined, the following results are obtained by the application of nonlinear regression method. (The detailed derivation of the following results are presented in the Appendix A.)

$$\underline{\underline{\Delta b}} = (\underline{\underline{F}}_b^T \underline{\underline{L}}^{-1} \underline{\underline{F}}_b)^{-1} \underline{\underline{F}}_b^T \underline{\underline{L}}^{-1} \underline{\underline{F}} \quad (\text{II-35})$$

$$\text{Var } \underline{\underline{b}} = (\underline{\underline{F}}_b^T \underline{\underline{L}}^{-1} \underline{\underline{F}}_b)^{-1} \sigma_F^2 \quad (\text{II-36})$$

$$\underline{\underline{\Delta p}} = \underline{\underline{F}}_p \underline{\underline{L}}^{-1} (\underline{\underline{F}} - \underline{\underline{F}}_b \underline{\underline{\Delta b}}) \quad (\text{II-37})$$

$$\sigma_p^2 = \frac{\underline{\underline{\Delta p}}^T \underline{\underline{A}}^{-1} \underline{\underline{\Delta p}}}{\Sigma S - k} = \frac{\Sigma (w_i \Delta p_i^2)}{\Sigma S - k} \quad (\text{II-38})$$

$$\sigma_{b_i}^2 = (\underline{\underline{F}}_b^T \underline{\underline{L}}^{-1} \underline{\underline{F}}_b)^{-1} \sigma_p^2 \quad (\text{II-39})$$

The calculational procedure is summarized as follows:

- (1) Assume the initial value of the virial coefficients and the approximate volume ratio for each isotherm of consecutive Burnett measurements.
- (2) With the assumed  $b_i$  and the measured pressure from the vector  $\underline{\underline{F}}$  and the matrices  $\underline{\underline{F}}_p$ ,  $\underline{\underline{F}}_b$ , and  $\underline{\underline{A}}$ .

- (3) Form the  $\underline{L}$  matrix from  $\underline{F}_p$  and the weighting matrix  $\underline{A}$ .
- (4) Invert the  $\underline{L}$  matrix.
- (5) Form the matrix of the normal equation  $\underline{F}_b^T \underline{L}^{-1} \underline{F}_b$ .
- (6) Calculate the corrections to the  $b_i$ .
- (7) With the new values of virial coefficients, repeat steps 1 to 6. Continue the iteration until coefficients are within some arbitrary small value of  $\Delta b_i$ .
- (8) Use the last step of the iteration to calculate the corrections to the pressure.
- (9) Use these corrections and the necessary statistical information from the matrices  $\underline{F}_p$ ,  $\underline{F}_b$ ,  $\underline{L}$ , and the normal equations to calculate the standard errors of estimate of the virial coefficients.

The above calculational procedure is an approximation to the exact, because  $\Delta p$  in equation (II-22) does not go to zero. The "exact" solution were developed by Britt and Luecke (9) and were programmed in Fortran using double precision arithmetic. The computer program is listed in Appendix D.

#### B. Regression Analysis to Obtain Constants of Benedict-Webb-Rubin Equation of State

Emperical equations of state are very useful for representating the experimental p-v-T surface of fluids. The Benedict-Webb-Rubin equation appears to be a reliable

expression in correlating experimental p-v-T data (3).

$$p = RT\rho + (B_0RT - A_0 - C_0/T^2)\rho^2 + (bRT - a)\rho^3 \\ + a\alpha\rho^6 + (c\rho^3/T^2)(1 + \gamma\rho^2)\exp(-\gamma\rho^2) \quad (\text{II-40})$$

In the compressibility factor form, this becomes,

$$Z = 1 + (B_0 - A_0/RT - C_0/RT^3)\rho + (b - a/RT)\rho^2 \\ + a\alpha\rho^5/RT + (c\rho^2/RT^3)(1 + \gamma\rho^2)\exp(-\gamma\rho^2) \quad (\text{II-41})$$

A method for evaluating these constants has been given by Brough et al. (10), and a computer program in Fortran language has been written by Dripps (15) to carry out the calculations. The parameters in Benedict-Webb-Rubin equation for fluoroform gas between 200°C and 350°C and pressure up to 150 atmosphere are presented in Table 1 and Table 2. This equation must be used with caution to extrapolate outside the range of the data.

## CHAPTER III

### EXPERIMENTAL APPARATUS AND PROCEDURE

The experimental apparatus constructed by Suh (55) and modified by Epperly (17) for obtaining p-v-T data of gases was used for this work. The dimensions of the Burnett cell as well as the volume ratio were changed. Helium gas was used to check the integrity and accuracy of the experimental equipment before obtaining the p-v-T data for fluoroform.

#### A. Experimental Apparatus

The Burnett cell consists of two separated volumes interconnected by an expansion valve and this is the heart of the experimental apparatus. The Burnett cell, the expansion valve, the charging system, the vacuum system, temperature control and measurement system, and the pressure measurement system are discussed in this section in that order. Schematic diagrams of the equipment installation are shown in Figure 1 and 2. The arrangement of the instruments are shown in photographs in Figure 5, 6, 7, and 8.

### The Burnett Cell

The detailed construction of the Burnett cell is shown in Figure 3. The cell consists of two cylindrical chambers,  $C_I$  and  $C_{II}$ . They were both made of 304 stainless steel. The over all length of the assembled cell was about 11 in. with an outside diameter of 4.5 in. and inside diameter of 1.6 in. The inside length of the top chamber was 5 in., the bottom was 2 in. Both chambers were welded closed with 1 in. thick ends and hydrostatically pressure tested after the first weld pass. This welded construction was necessary to eliminate of any possible leaks and to minimize the distortion of the vessels as pressure was applied. Three ports were put in the top chamber for connecting the charging line, the differential pressure cell, and the expansion valve. A thermal well was drilled into the wall of the top chamber for insertation of a platinum resistance thermometer for the temperature measurements. Two ports were put into the bottom chamber. One connected to the expansion valve and the other to the vacuum system. The Burnett cell and all connecting tubing were thoroughly cleaned by washing with cleaning solution and acetone before final assembly. Two high temperature valves with extended bonnets were used as block valves for charging the system gas into chamber  $C_I$  and for evacuating the chamber  $C_{II}$ .

### The Expansion Valve

The expansion valve used in this work was designed in this laboratory. This bellows type valve provides positive leak-tight closure after each expansion. Figure 4 is a schematic diagram of the expansion valve.

The type 321 stainless steel bellows was 15/32 in. O.D. and 0.456 in. I.D. and had a 0.0045 in. wall thickness. The bellows had 14 convolutions with a maximum stroke of 0.056 in. This bellows was silver soldered to the valve stem and to the base of the valve. The valve bonnet was about 11 in. long. Both the valve body and the stem were made of type 316 stainless steel.

Clean, dry nitrogen was introduced into the upper part above the bellows to equalize the pressure differential across the bellows. "Teflon" packing is provided at the top of the bonnet to prevent the loss of nitrogen from the pressure transmitting system. Standard  $\frac{1}{4}$  in. high pressure tubing was welded to the valve ports which connected the valve to the Burnett cell  $C_I$  and  $C_{II}$ , and the nitrogen pressure system.

### The Charging System

The charging system as shown in Figure 1 was capable of charging the system gas from gas cylinder supply pressure up to 8,000 psi using a hand operated mercury positive displacement pump (MP). The hand-pump was a Ruska model

2250 positive displacement pump with a capacity of 250 cc. Initially, the system gas was charged into the surge tank (ST) as well as the Burnett cell  $C_I$ . Higher pressures were obtained with the mercury hand pump. The surge tank made of type 304 stainless steel had a volume of 19 cubic in., and was designed for a working pressure of 10,000 psia (55). The mercury level in the surge tank was calibrated against the mercury level in the mercury reservoir (MR) of the hand pump. Mercury accidentally carried over was collected in the mercury trap (MT). To prevent this carry over, a mercury indicator (MI) was installed in the charging line between the surge tank and the mercury trap. The mercury trap was a stainless steel vessel located between the surge tank and the Burnett cell  $C_I$ . The mercury indicator was made of type 304 stainless steel and has two leads connected to a DC battery and a warning light in series. When the light came on the mercury level had reached the probe level and the pumping was stopped. A high temperature block valve isolating the charging system from the Burnett cell was submerged in the constant temperature bath. Standard high pressure valves (rated at 30,000 psi) and  $\frac{1}{4}$  in. O.D. by 0.083 in. I.D. high pressure tubing (rated at 60,000 psi) were used to construct the charging system.

### The Vacuum System

The vacuum system attached to the apparatus consisted



of a Welch Scientific Duo-Seal, Model 1402B vacuum pump (VP) and a Virtus McLeod vacuum gauge (MG). The pumping rate was of 150 liters/min. in free air. It took less than 10 minutes to evacuate the whole system to 50 microns (0.05 torr). The low pressure vacuum was measured with the Virtus McLeod vacuum gauge. The McLeod vacuum gauge had a scale reading from 0.005 torr to 5 torr.

There was another vacuum system attached to the low pressure air lubricated dead weight gauge. The pump attached to this vacuum system was a Precision Scientific Model 75 vacuum pump. The pumping rate was 70 liters/min. in free air. An Ace McLeod vacuum gauge with a scale reading of 0.01 to 10 torr was attached to this system. This vacuum system served as the reference pressure when making the atmospheric pressure measurements through the low-pressure range air lubricated piston gauge.

### Temperature Control and Measurement System

The Burnett cell  $C_I$ ,  $C_{II}$ , the expansion valve, two high temperature block valves, and the high temperature differential pressure indicator cell were all submerged in the constant temperature bath. The bath temperature was controlled by a Hallikainen Model 1053A Thermotrol (TC), with a resistance thermometer sensing elements ( $RT_2$ ) and two 125 watts adjustable internal heaters.

The constant temperature bath was made of stainless

steel tank of 18 in. in diameter and 30 in. deep with a capacity of about 4 cubic feet of fluid. A thin asbestos cloth was wrapped around the bath tank to electrically insulate the tank from the resistance heating wire. Four fixed and one adjustable external heaters were wound around the bath tank. Each of these external heaters were made of 40 feet of A.W.G. No. 20 Chromel-A asbestos insulated wire with resistance of 0.6375 ohms/ft., the power to the heaters was controlled by individually fused circuitd.

The bath tank and the heater assembly was insulated by 6 in. of insulating material and held in place by an outer jacket made of 24 ga. stainless steel tank.

The bath fluid was a mixture of 40% sodium nitrite, 53% potassium nitrate and 7% sodium nitrate by weight which melts at about 140°C. The bath fluid was circulated by two draft tube, down flow stirrers. The sterrers were driven at 1725 rpm by induction motors.

The desired coarse adjustment of the bath temperature was first made by using one or more of the five external heaters. The final temperature was controlled by the Thermotrol temperature controller that operate the internal heaters. It was possible to control the temperature of the bath within  $\pm 0.001^{\circ}\text{C}$  of the desired set point temperature over the full range of these measurements. The temperature changes of  $0.001^{\circ}\text{C}$  could be easily detected.

The temperature of the gas in the Burnett cell was measured by a National Bureau of Standards calibrated

platinum resistance thermometer ( $RT_1$ ) inserted into a thermometer well in the wall of the Burnett cell  $C_I$ . The resistance of the thermometer was measured by a Mueller Bridge (MB) coupled to an optical Galvanometer (GA) and this resistance converted into the temperature reading.

### Pressure Measurement System

The pressure in the system was measured with dead weight gauges (DWG) manufactured by Ruska Instrument Corp. Two oil lubricated dead weight gauges and two air lubricated dead weight gauges were installed during the previous experiment. The low-pressure oil lubricated dead weight gauge ( $DWG_L$ ) range from 6 to 2428 psig. The high-pressure oil lubricated dead weight gauge ( $DWG_H$ ) range from 30 to 12,140 psig. The high-pressure air lubricated dead weight gauge ( $APG_H$ ) range from 2 to 600 psig. The low-pressure air lubricated dead weight gauge ( $APG_L$ ) range from 0.2 to 15 psig. Detailed descriptions of these dead weight gauges are given in Appendix B.

In this work the general range of the system pressure was between 20 to 2,300 psig. The system pressure was measured with the low-pressure oil lubricated dead weight gauge. Atmospheric pressure was measured with the low-pressure air lubricated dead weight gauge and with a mercury barometer located near the Burnett apparatus. These barometric pressure reading was used to convert the pressure

measured by low-pressure oil lubricated dead weight gauge to absolute pressure. All pressure measurements were subject to corrections due to room temperature changes, elastic distortion of the pistons, local accelerating gravity, and buoyancy. Details of these corrections are given in the Appendix C.

Measuring the pressure of the system gas in the Burnett cell was the main purpose of this project. The transmission of the gas pressure to the dead weight gauge consisted of an elaborate piping system. A schematic diagram of the pressure measuring system is shown in Figure 1.

Two sets of the differential pressure indicators (DPI) were used in the pressure measurement system. The high temperature differential pressure indicator was submerged in the constant temperature bath and this separated the system gas from the pressure transmitting fluid. The pressure of the system gas was sensed by a thin stainless steel diaphragm located in the high temperature differential cell. A differential pressure across the diaphragm caused the diaphragm to deflect which changed the core-coil position in a linear differential transformer. This motion was shown by the electronic null indicator. The linear differential transformer was located at the top of the differential pressure cell outside of the constant temperature bath for the protection of the electronic components. Clean, dry nitrogen gas served as the pressure transmitting fluid.

The system gas pressure was balanced by the adding or removing nitrogen gas with a hand operated mercury positive displacement pump.

A second differential pressure cell is used to separate the nitrogen gas from the oil in the oil lubricated dead weight gauge system. A second differential pressure null indicator was attached to the differential pressure cell for adjusting the differential pressure across the diaphragm of the differential pressure cell. A reference manometer was placed in the oil line between the dead weight gauge and the differential pressure cell indicating the reference oil level.

A Heise gauge was attached to the sample gas system to give an approximate reading of the initial gas pressure in the Burnett cell. This approximate pressure could be adjusted by a Ruska Model 2250 hand operated positive displacement mercury pump. Two Heise gauges were attached to the nitrogen gas system to permit close estimates of the weight loads for the dead weight gauges and to balance the pressure in the bellows of the expansion valve.

Two Ruska Model 2426.1 hand operated positive displacement mercury pumps were attached to the nitrogen gas system and the oil system, respectively. These pumps are used for the necessary pressure adjustments.

Standard high pressure stainless steel  $\frac{1}{4}$  in. O.D. tubing and high pressure valves were used through the pressure measurement system.

## Safety Precautions

All of the electrical equipment was protected by circuit breakers or time-delay fuses located in the power control panel. The constant temperature bath was protected by a Fenwal Thermoswitch (FT) located in the constant temperature bath and set at  $390^{\circ}\text{C}$ . Power to the electrical control panel was cut off if the bath temperature went above this preset thermoswitch temperature. Two remote cutoff switches were located outside the laboratory for emergency power shut down. Power to the circuits of the system were controlled by the power switch located on the control panel.

## B. Experimental Procedure

Before operation the whole system was pressure tested by charging the helium gas into the system to 2,000 psi. When the helium in the test system and the nitrogen in the pressure transmission system remained for three days with no detectable leaks, the system was assured to be free of leaks.

The procedure for one series of pressure expansion on an isotherm using the Burnett method is described below. All expansion series were run according to this procedure.

1. The heat transfer salt in the constant temperature bath was melted with the external heaters.
2. The constant temperature bath was then lifted into position. The bath fluid was circulated with the two

stirrers in the bath tank. An air blower was used to cool the electronic components at the top of the high temperature differential pressure cell.

3. When the predetermined isotherm temperature was approached, the thermotrol was turned on. The coarse control setting of the thermotrol was set to a point close to the predetermined temperature set point.
4. The final temperature was controlled by the adjustment of the fine control setting of the thermotrol. It took about 30 hours to attain the predetermined isotherm from the time power was turned on to melt the salt.
5. Good room temperature control was a very important factor in controlling of bath temperature. The temperature of the room was controlled within  $\pm 0.5^{\circ}\text{C}$ .
6. The bath temperature was measured with a platinum resistance thermometer, mueller bridge, and galvanometer with optical scaling reading device. The thermometer resistance indicated on the mueller bridge were converted to temperature reading.
7. When the bath temperature had remained constant for a period of at least 60 minutes, the electronic indicator on the high temperature differential pressure cell was zero adjusted by venting both sides of the differential pressure cell to atmosphere. This procedure was necessary on each isotherm to eliminate the possible zero shift due to thermal expansion.

8. The entire system was evacuated to less than 0.05 torr. The system was flushed with the test gas and evacuated again. This flush-evacuation sequence was repeated three times to insure a clean system.
9. Nitrogen gas and the test gas were introduced into the system simultaneously. Keeping the pressure difference between the system gas and the nitrogen gas within 50 psi to prevent over pressuring the bellows of the expansion valve. This safety range could be easily controlled within the 50 psi limit.
10. The nitrogen gas pressure was kept slightly higher than the test gas pressure. The diaphragm of the differential pressure cell then deflected in one direction only. This eliminated any zero shift due to deformation of the diaphragm that occurs when the diaphragm is over-pressured from both sides.
11. Pressure balance was attained by adding or venting nitrogen gas. Weights were placed on the dead weight gauge until both the differential pressure null indicators were nulled.
12. At the balance point, the weights on the dead weight gauge, the temperature of the Burnett chamber, the room temperature, the barometric pressure, and the time of the day were all recorded.
13. The expansion valve was slowly opened to allow the test gas to expand into the preevacuated chamber  $C_{II}$ . Precautions were taken to prevent the pressure difference



between the test gas and the nitrogen gas from exceeding 100 psi in order to protect the bellows of the expansion valve.

14. When thermal equilibrium was restored after the expansions, the expansion valve was closed.
15. Steps 11 and 12 were repeated until the pressure remained constant.
16. The valve to the vacuum pump was closed when the chamber  $C_{II}$  gas was vented to atmosphere outside of the laboratory building. The vent was then closed and the chamber  $C_{II}$  was again evacuated to less than 0.05 torr. The pressure measurement on chamber  $C_I$  were observed during the venting and evacuation process to check for any possible leaks through the expansion valve. This pressure must remain constant during the evacuation of  $C_{II}$ .
17. About one hour was required to make each expansion. Successive expansions were obtained by repeating steps 13 to 16 until the test gas pressure down to about 30 psi.
18. This completed one series of isothermal expansions. About 12 expansions were required to expand from the initial pressure of 2,200 to about 30 psi.

The experimental data obtained are recorded in Appendix E.

## CHAPTER IV

## RESULTS AND DISCUSSIONS

A. Calibration of Burnett Cell with Helium

The performance of the Burnett apparatus was tested by taking p-v-T measurements on helium on the 200, 250, 300, and 350°C isotherms. Helium was used as the calibrating gas because accurate p-v-T data are available in the literature. It also has nearly a linear isotherm on the  $p_{r-1}/p_r$  versus  $p_r$  curve which makes it much easier to obtain the instrument constant. This constant should be close to but not necessarily the same as the instrument constant for another gas. The original experimental data for helium are presented in Table E-1 of the Appendix E. The second and the third virial coefficients, the apparatus constants with the standard error of estimate obtained from the helium measurements are presented in Table 3. The average values of the second, the third virial coefficients and the standard errors of estimate for each isotherm are presented in Table 4. The second virial coefficients for helium are compared with the values reported by other investigators in Table 5. The agreement between these values is within the experimental error of this experimental method.

## B. Fluoroform Data

Experimental measurements on fluoroform were made at pressure up to 150 atmosphere over the temperature range from 200°C to 350°C at 50°C intervals. Two runs were made on each isotherm. The original experimental data are presented in Table E-1 of the Appendix E. The nonlinear regression method described in Chapter II was used to calculate the second and the third virial coefficients. The results of these calculations and the standard error of estimate are presented in Table 6. The average values of the second and the third virial coefficients with the standard error of estimate for each isotherm are presented in Table 7. The virial coefficients versus temperature plots are presented in Figure 9 and 10. No data were found in the literature in the 200 to 350°C range to compare with the second and the third virial coefficients obtained from this work. The available low temperature second virial coefficients are shown on Figure 9 for comparison with the high temperature values. No values of the third virial coefficients were reported.

The method described in Chapter II was used to calculate the compressibility factors of fluoroform at each data point. The run constant of each series of expansions and the experimental compressibility factors for fluoroform at each data point are presented in Table 8. Compressibility factors calculated from the Benedict-Webb-

Rubin equation of state reproduce these experimental values well within the experimental error of the data in the range between 200°C and 350°C and up to 150 atmospheres.

### C. Error Analysis

The inherent errors in the Burnett experiment are those associated with the measurement of the temperature, the pressure, and those arising from uncertainties in the nonlinear regression analysis.

The measurement errors are those assignable to the instruments used. The uncertainties due to the incomplete evacuation of the lower cell before each expansion, the temperature variations during each run must be accounted for, and the errors in the pressure measurements must be assigned.

The effect of these assignable errors on the compressibility factor are defined as follows; with  $Z$  defined by

$$Z = \frac{pv}{nRT} = \frac{p}{\rho RT} \quad (\text{IV-1})$$

A virtual change in  $Z$  is given by,

$$dZ = \left( \frac{\partial Z}{\partial p} \right) dp + \left( \frac{\partial Z}{\partial T} \right) dT + \left( \frac{\partial Z}{\partial \rho} \right) d\rho \quad (\text{IV-2})$$

Computing the coefficients in equation (IV-2),

$$(\partial Z / \partial p) = 1 / \rho RT$$

$$(\partial Z / \partial T) = -(p / \rho RT^2) \quad (IV-3)$$

$$(\partial Z / \partial \rho) = -(p / \rho^2 RT)$$

Substituting equation (IV-3) into equation (IV-2), and rearranging,

$$dz = \left( \frac{1}{\rho RT} \right) dp - \left( \frac{p}{\rho RT^2} \right) dT - \left( \frac{p}{\rho^2 RT} \right) d\rho \quad (IV-4)$$

The assignable error was obtained by taking the absolute value of each term of equation (IV-4),

$$dz = \left| \left( \frac{1}{\rho RT} \right) \right| dp + \left| \left( \frac{p}{\rho RT^2} \right) \right| dT + \left| \left( \frac{p}{\rho^2 RT} \right) \right| d\rho \quad (IV-5)$$

The relative error was obtained by dividing equation (IV-5) by equation (IV-1),

$$\frac{|dz|}{Z} = \frac{|dp|}{p} + \frac{|dT|}{T} + \frac{|d\rho|}{\rho} \quad (IV-6)$$

The assignable error in pressure measurements were in the range,  $0.030\% \leq dp/p < 0.049\%$ .

The maximum temperature variation during each run was  $0.0055^\circ\text{C}$ . This uncertainty in the temperature

measurement will contribute less than 0.03% error to the calculation of compressibility factors. The assignable errors in the temperature measurement were in the range,  $0.006\% \leq dT/T < 0.003\%$ .

The maximum uncertainty due to the incomplete evacuation Burnett cell  $C_{II}$ , before each expansion were less than 0.0035%. The assignable errors due to the incomplete evacuation of Burnett cell were in the range,  $4.3 \times 10^{-5}\% \leq dP/P < 0.0035\%$ .

The total assignable error contributed to the calculation of compressibility factors were in the range,  $0.037\% \leq dZ/Z < 0.056\%$ .

## CHAPTER V

## CONCLUSIONS AND RECOMMENDATIONS

A. Conclusions

The Burnett apparatus is a very useful way to obtain highly accurate pressure sequences which can be used to determine the gas compressibility factors and the virial coefficients in the virial equation of state for gases. The Burnett apparatus in this laboratory can be operated to 8,000 psi and in the temperature range of 200°C and higher.

Measurements were made on helium and fluoroform between 200°C and 350°C at a 50°C intervals and pressures up to 150 atmosphere. From this measurements, the following conclusions can be drawn:

- (1). The second virial coefficients of the helium were in good agreement with the values reported by a number of other investigators. This indicates the present equipment is reliable for obtaining accurate p-v-T data.
- (2). At 200, 250, 300, and 350°C the second and the third virial coefficients of fluoroform gas were calculated from the Burnett p-v-T measurements. These represent new experimental results.

- (3). The parameters for the Benedict-Webb-Rubin equation were obtained by fitting the experimental Burnett p-v-T data. The Benedict-Webb-Rubin equation represent the data within 99.99% confidence level based on the standard estimate of error between the computed and the experimental values. The compressibility factors computed with the Benedict-Webb-Rubin equation are within experimental error for all data points for the fluoroform gas over the temperature between 200 and 350°C and pressure to 150 atmosphere.

#### B. Recommendations

The following suggestions are made for future work:

- (1). From a review of literature, p-v-T measurements of fluoroform gas are available only from 0 to 130°C. It would be useful to obtain compressibility factors and the second and the third virial coefficients for fluoroform gas in this lower temperature range. In order to do this, the heat transfer salt in the constant temperature bath would have to be replaced by commercially available heat transfer oil. Physical adsorption as well as chemisorption of the fluoroform on the Burnett cell wall may be a problem when using the Burnett apparatus for p-v-T measurements at these lower temperature level. Both theoretical and experimental suggestions has been



made by several investigators (1,20,25,45) to overcome these adsorption effects. A careful review of these papers is recommended before this work proceeds.

- (2). Evaluation of the second and the third virial coefficients of a selected binary gas mixture at moderate and high temperature levels would be a worthwhile experiment, this would supplement data that are available at low temperature.
- (3). The  $p_{r-1}/p_r$  versus  $p_r$  plot of the experimental data points shows scatter of the data points when the experimental pressure is less than 100 psi. This may be due to reduced sensitivity of the high temperature differential pressure cell in this lower pressure range. Careful inspection and analysis of the design of these cells to possibly improve the performance is recommended.
- (4). The assignment of the weighting factor in equation (II-33) is arbitrary and the detailed functional form that factor should take is unknown. Because the error in each pressure measurement is nearly constant over the pressure range of this work, an a priori assignment of the weighting factor suggests  $w_i = (p_i)^2$ . The simplest empirical correction to this weighting factor is a linear translation of the pressure so that  $w_i = (p_i + a)^2$  where the "best value" of  $a$  is selected by minimizing the standard error of estimate. Because the third virial coefficient is so sensitive to the

"best fit", it is recommended that the functional form of this weighting factor be examined and additional empirical procedures be used to study the effect of the weighting of the experimental data.

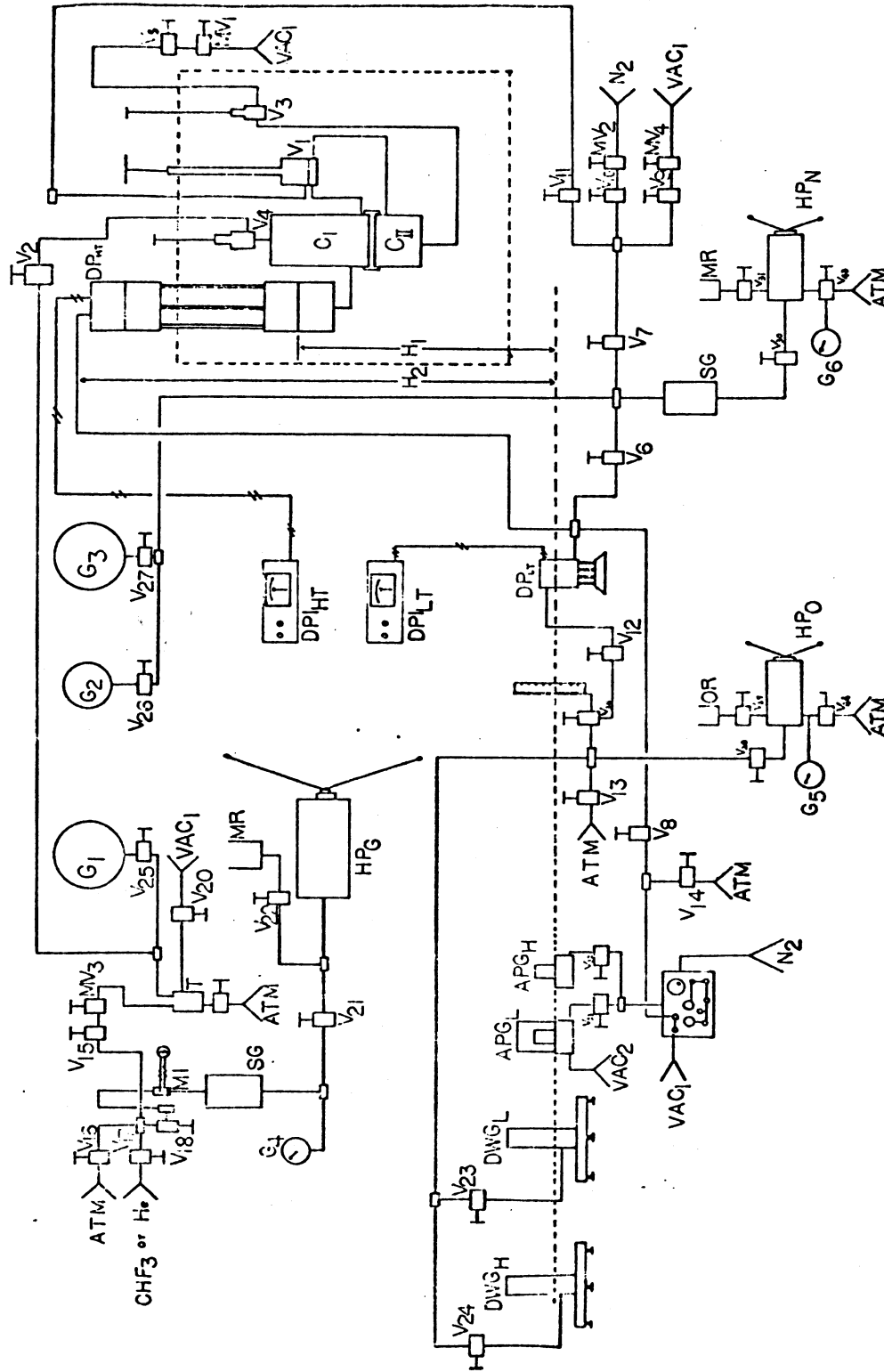


Figure 1. Schematic Diagram of Pressure Measurement and Charging System

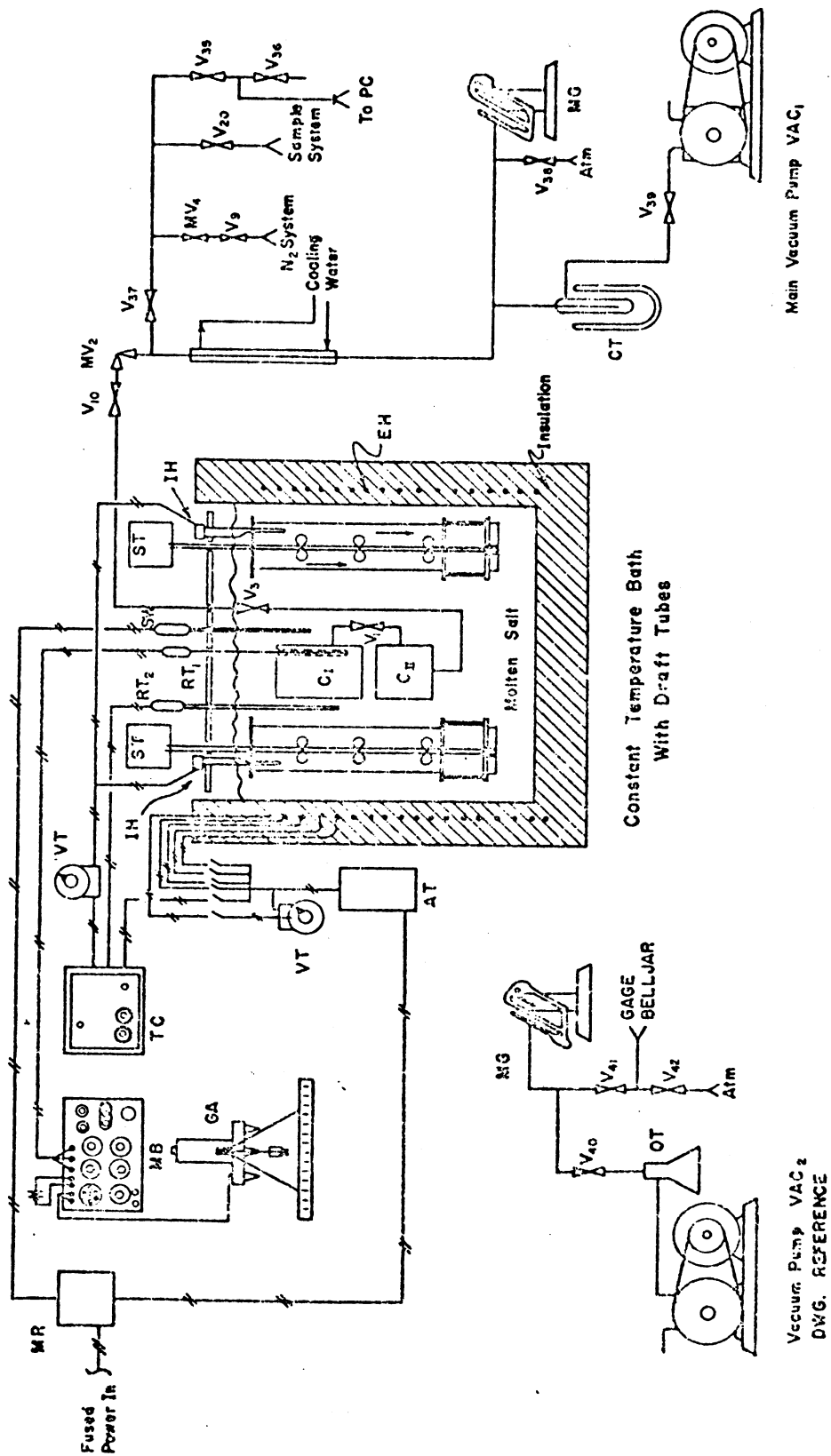


Figure 2. Schematic Diagram of Thermal and Vacuum System

## LIST OF SYMBOLS USED IN FIGURES

APG <sub>H</sub>	High range air piston gauge 6 - 600 psig
AOG <sub>L</sub>	Low range air piston gauge 0.4 - 15 psig
AT	Auto transformer
C <sub>I</sub>	Upper Burnett cell
C <sub>II</sub>	Lower Burnett cell
CT	Cold trap
DP <sub>HT</sub>	High temperature differential pressure cell
DP <sub>LT</sub>	Low temperature differential pressure cell
DPI <sub>HT</sub>	High temperature differential pressure indicator
DPI <sub>LT</sub>	Low temperature differential pressure indicator
DWG <sub>H</sub>	High range dead weight gauge 30 - 12,140 psig
DWG <sub>L</sub>	Low range dead weight gauge 6 - 2,428 psig
EH	External heater
G <sub>1</sub>	Heise gauge 0 - 5,000 psig
G <sub>2</sub>	Heise gauge 0 - 100 psig
G <sub>3</sub>	Heise gauge 0 - 5,000 psig
GA	Galvanometer, scale, and light source
H <sub>1</sub>	Elevation of high temperature dead weight gauge diaphragm from reference plane
H <sub>2</sub>	Elevation of the highest point in pressure transmitting tubing from reference plane
HP <sub>O</sub>	Hand pump for DWG oil
HP <sub>G</sub>	Hand pump, mercury, sample charging

HP <sub>N</sub>	Hand pump, mercury, nitrogen system
IH	Internal heater
MB	Mueller bridge
MI	Mercury indicator
MR	Mercury reservoir in Fig. 1 Magnetic relay in Fig. 2
MV <sub>1</sub>	Sample discharge flow control valve
MV <sub>2</sub>	Nitrogen charge flow control valve
MV <sub>3</sub>	Sample charge flow control valve
MV <sub>4</sub>	Nitrogen discharge flow control valve
OT	Oil trap
PC	Pressure control pack
RT <sub>1</sub>	Resistance thermometer for temp measurement
RT <sub>2</sub>	Resistance thermometer for temp control
SG	Surge tank
ST	Bath stirrers
SW	Fenwal thermal protect switch
T	Mercury trap
TC	Temperature controller
VAC <sub>1</sub>	Main vacuum system
VAC <sub>2</sub>	Vacuum system for APG <sub>L</sub>
VT	Variable transformer
V <sub>1</sub>	Expansion valve
V <sub>2</sub>	Sample charge isolation valve
V <sub>3</sub>	Sample isolation valve discharge side
V <sub>4</sub>	Sample isolation valve charge side
V <sub>5</sub>	Sample discharge isolation valve

V <sub>6</sub>	Nitrogen system isolation valve
V <sub>7</sub>	Nitrogen system isolation valve
V <sub>8</sub>	System pressure to control pack isolation valve
V <sub>9</sub>	Nitrogen system vacuum shut off valve
V <sub>10</sub>	Nitrogen system source shut off valve
V <sub>11</sub>	Nitrogen system shut off for bellows side
V <sub>12</sub>	Oil system DP <sub>LT</sub> isolation valve
V <sub>13</sub>	Oil bleed valve
V <sub>14</sub>	Control pack to atmosphere valve
V <sub>15</sub>	Sample charging shut off valve
V <sub>16</sub>	Sample source shut off valve
V <sub>17</sub>	Helium source shut off valve
V <sub>18</sub>	Mercury surge cut off valve
V <sub>19</sub>	Mercury trap drain valve
V <sub>20</sub>	Sample system vacuum shut off valve
V <sub>21</sub>	Charging pump outlet valve
V <sub>22</sub>	Charging pump inlet valve
V <sub>23</sub>	DWG <sub>L</sub> isolation valve
V <sub>24</sub>	DWG <sub>H</sub> isolation valve
V <sub>25</sub>	G <sub>1</sub> isolation valve
V <sub>26</sub>	G <sub>2</sub> isolation valve
V <sub>27</sub>	G <sub>3</sub> isolation valve
V <sub>28</sub>	Oil pump outlet valve
V <sub>29</sub>	Oil pump inlet valve
V <sub>30</sub>	Nitrogen pump outlet valve
V <sub>31</sub>	Nitrogen pump inlet valve

V<sub>32</sub> APG<sub>H</sub> isolation valve  
V<sub>33</sub> APG<sub>L</sub> isolation valve  
V<sub>34</sub> Three way valve for oil head reference  
V<sub>35</sub> Pressure control pack vacuum shut off valve  
V<sub>36</sub> Atmosphere bleed valve  
V<sub>37</sub> Vacuum isolation valve  
V<sub>38</sub> Atmosphere bleed valve  
V<sub>39</sub> Vacuum pump #1 isolation valve  
V<sub>40</sub> Vacuum pump #2 isolation valve  
V<sub>41</sub> Vacuum pump to bell jar isolation valve  
V<sub>42</sub> Vacuum system #2 atmosphere bleed valve  
V<sub>43</sub> Nitrogen hand pump atmosphere bleed valve  
V<sub>44</sub> Oil hand pump atmosphere bleed valve



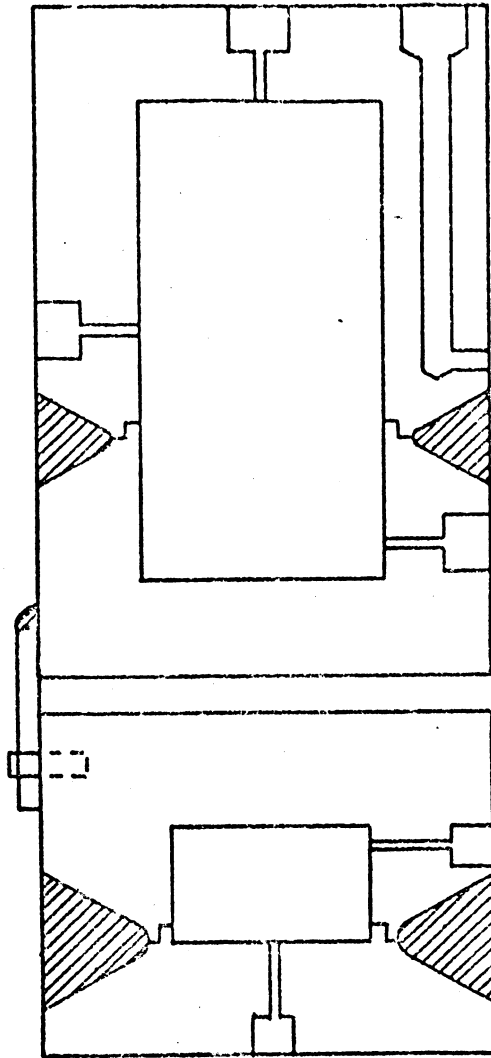


Figure 3. The Burnett Cell

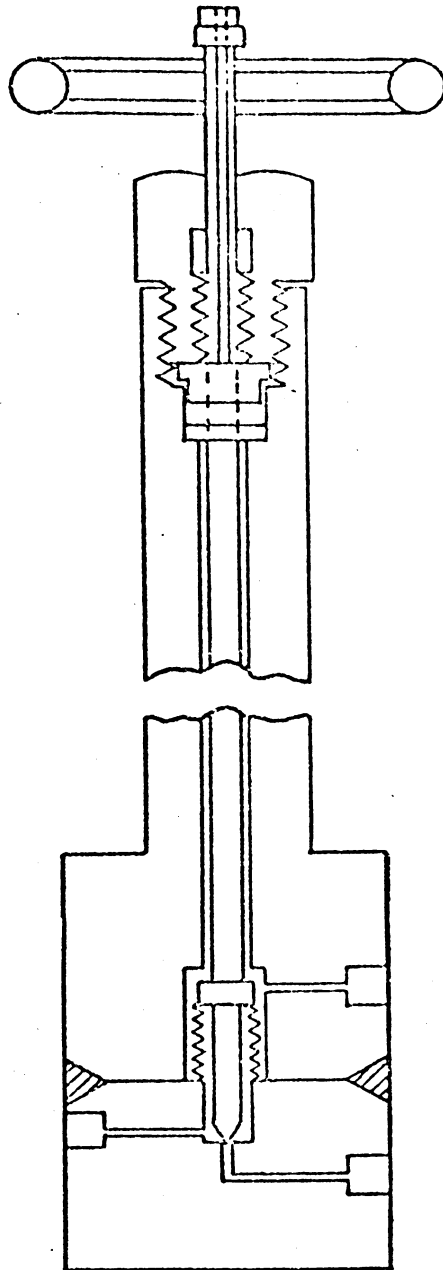


Figure 4. The Expansion Valve

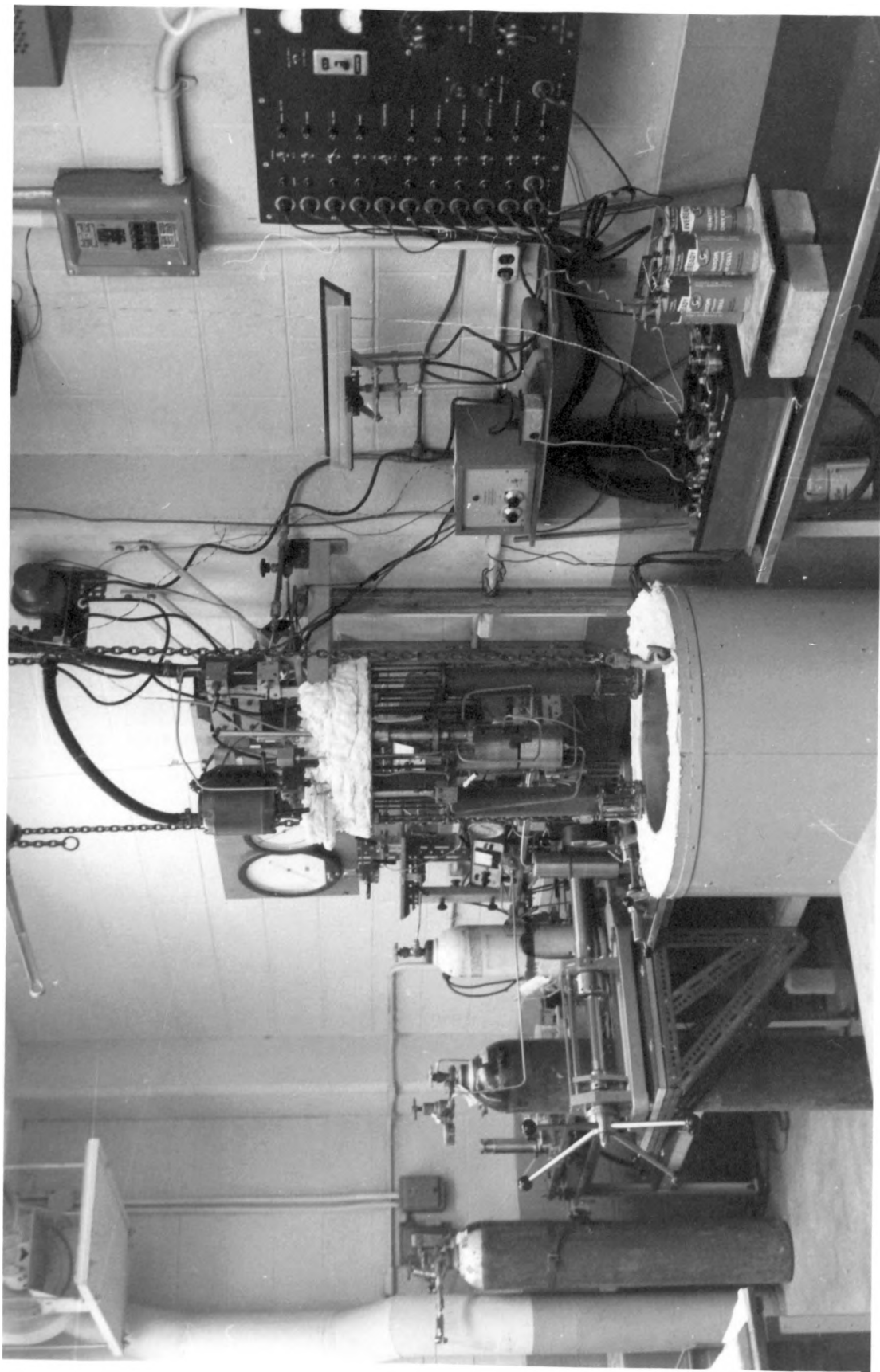


Figure 5. The Experimental Apparatus

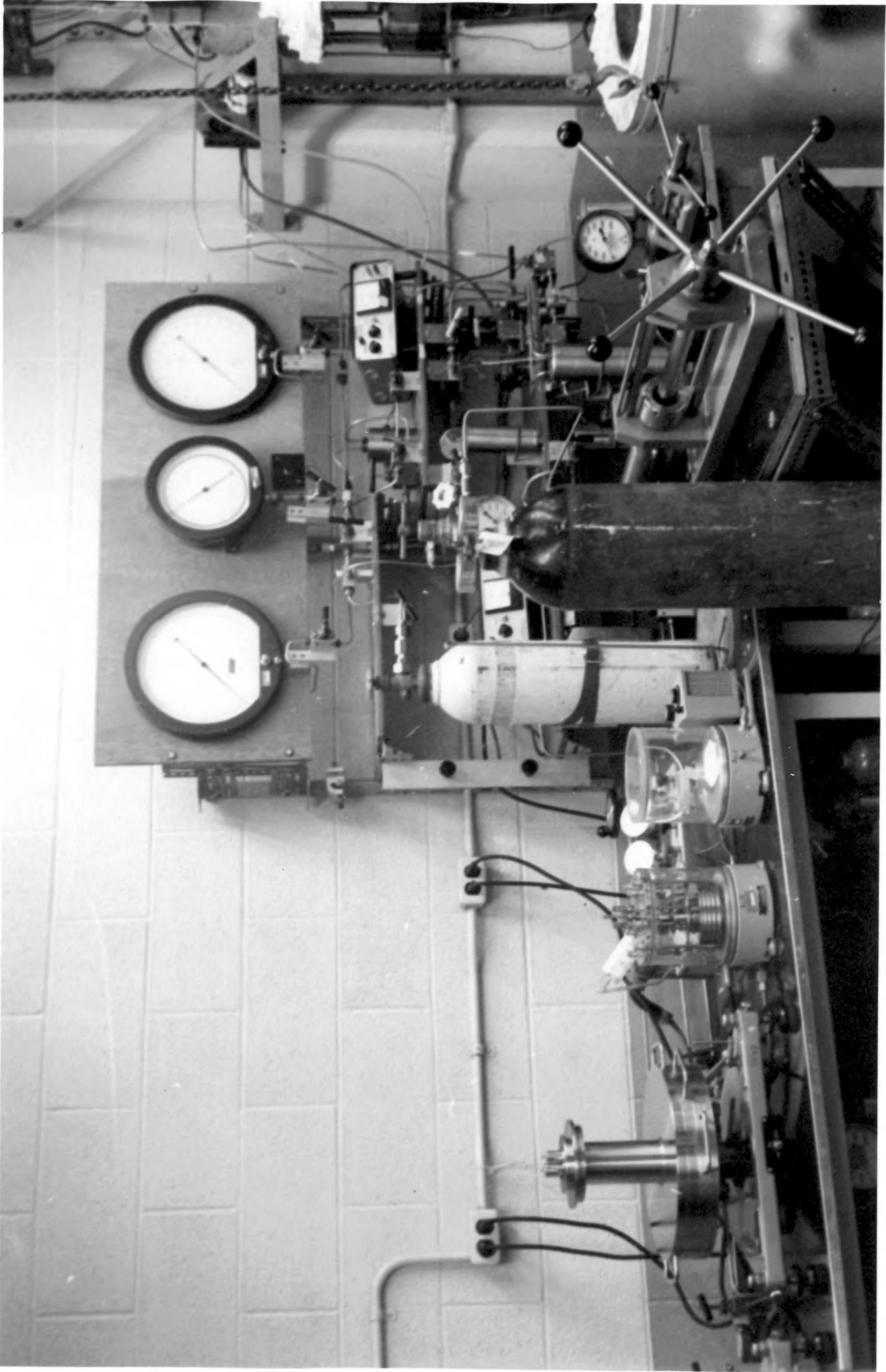


Figure 6. Pressure Measurement Devices

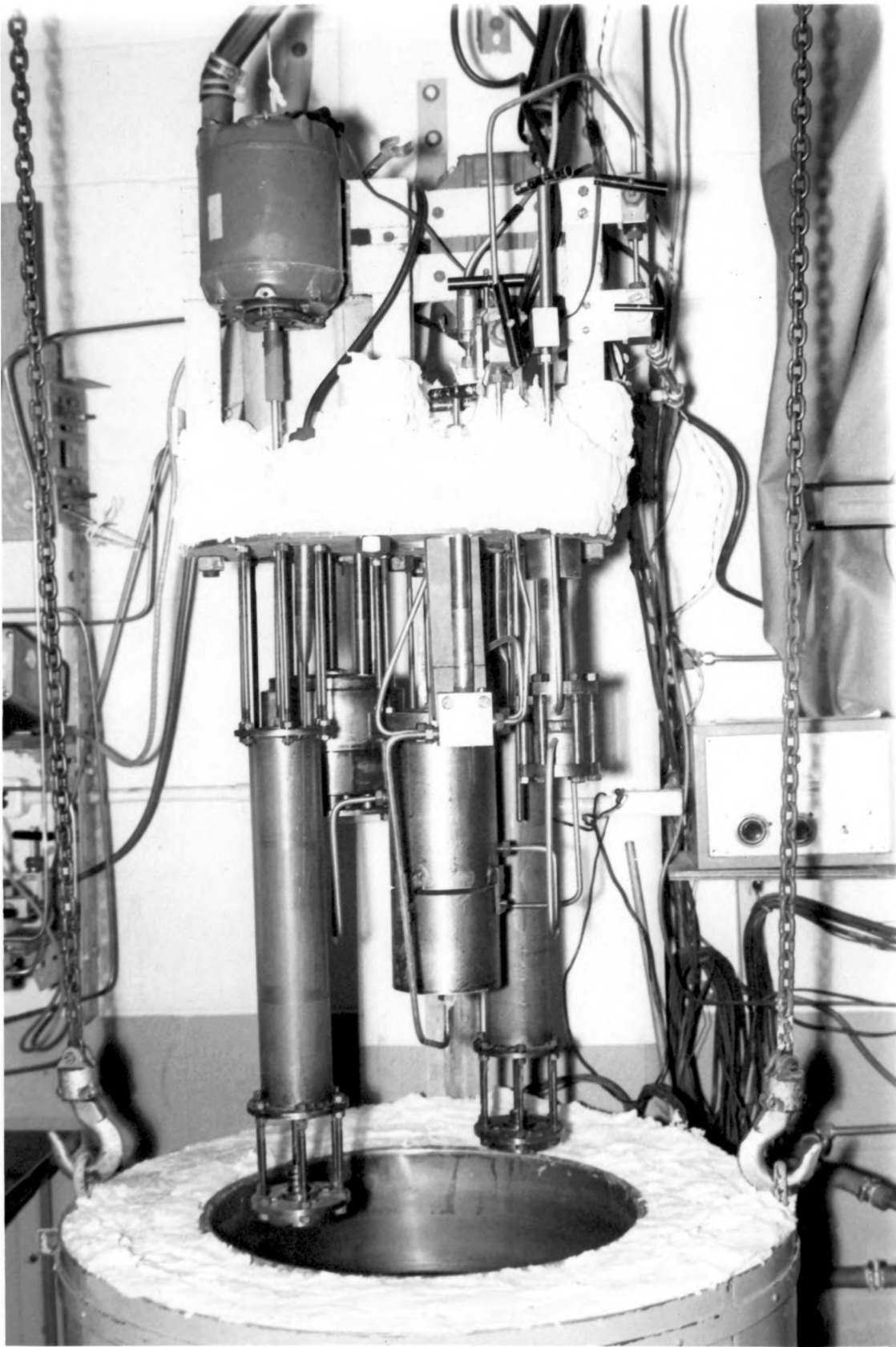


Figure 7. The Contents of the Constant Temperature Bath

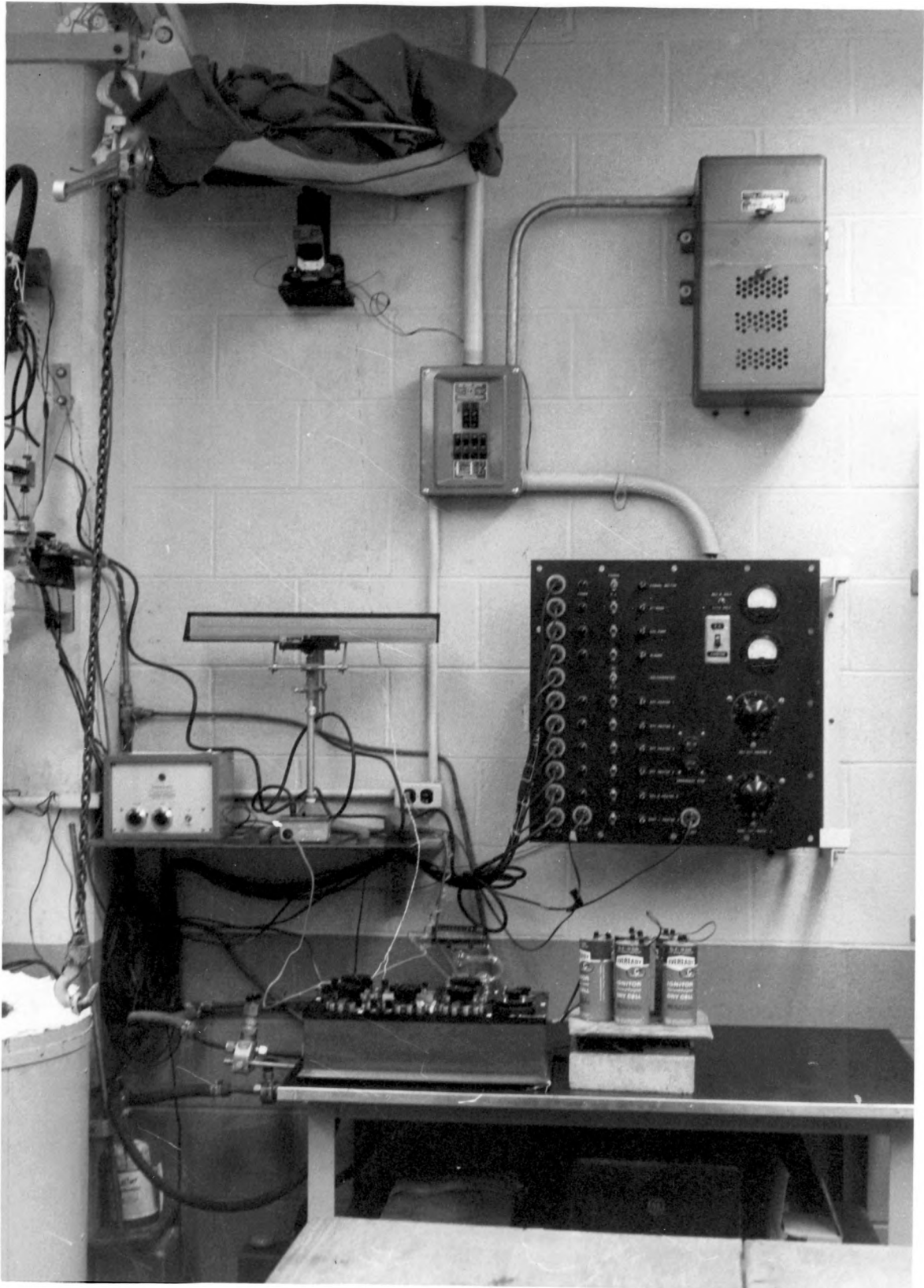


Figure 8. Temperature Control and Measurement Devices

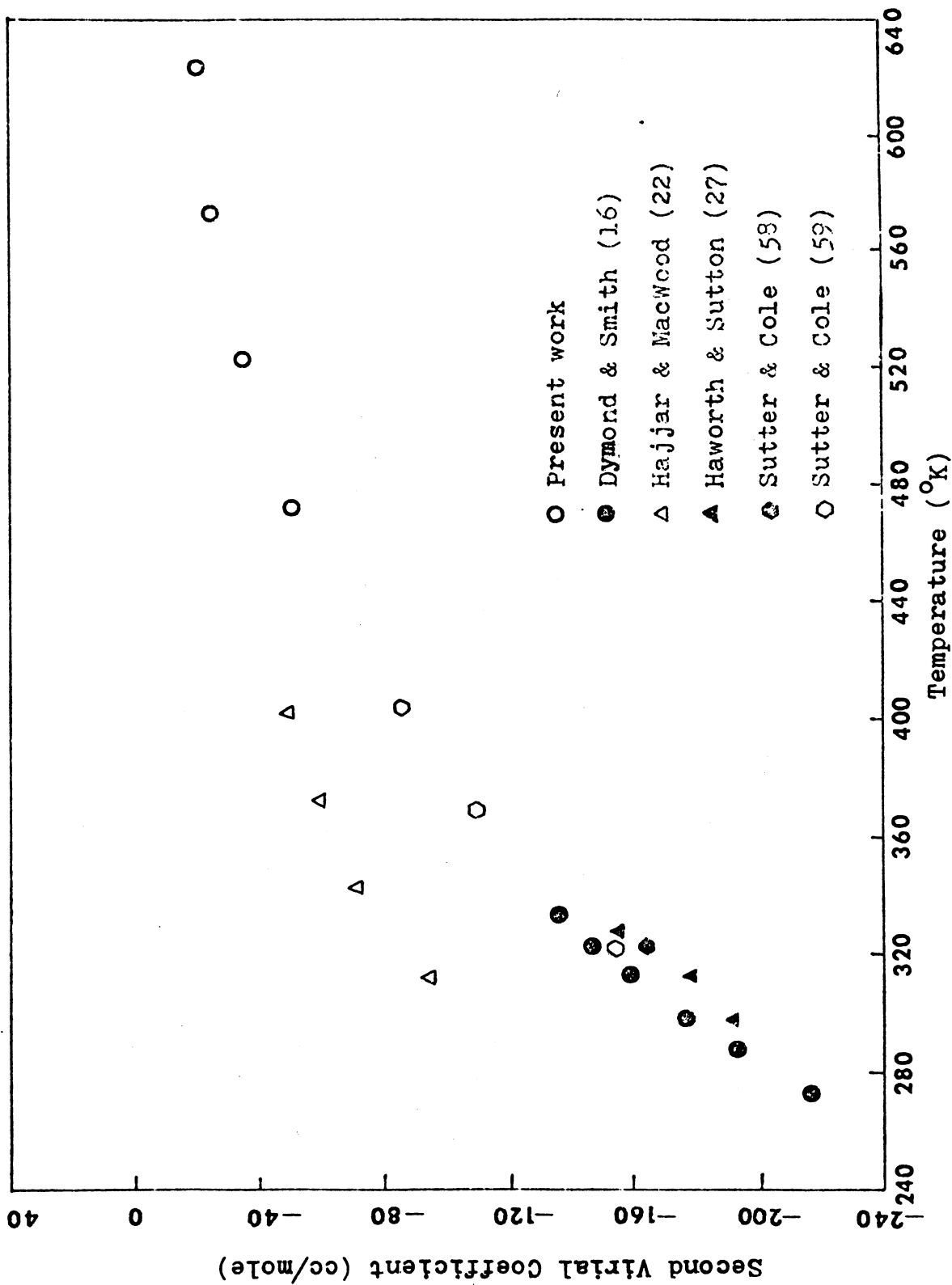


FIGURE 9. TEMPERATURE VERSUS SECOND VIRIAL COEFFICIENTS OF FLUOROFORM

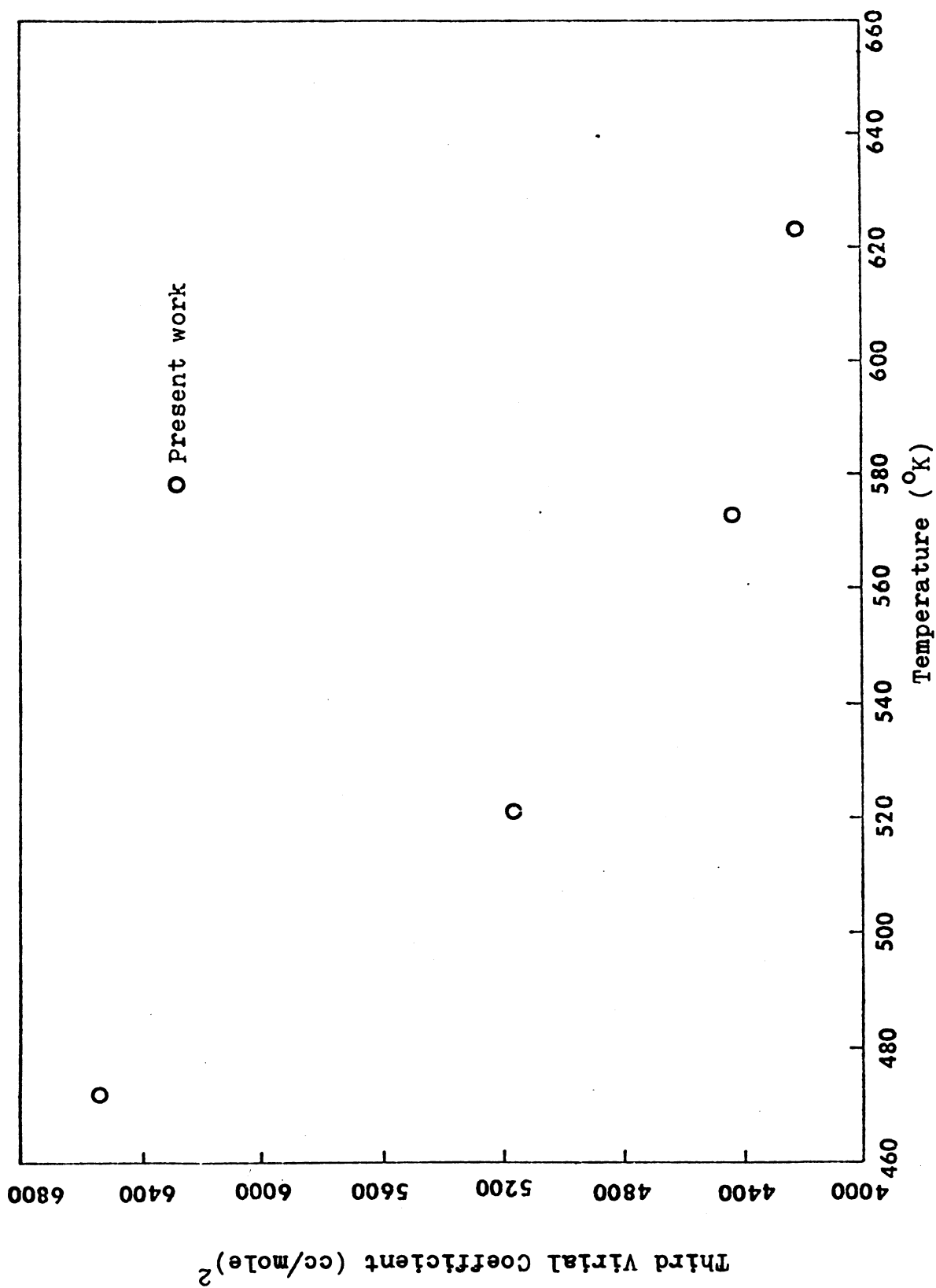


FIGURE 10. TEMPERATURE VERSUS THIRD VIRIAL COEFFICIENTS OF FLUOROFORM



TABLE 1

NUMERICAL VALUES OF THE CONSTANTS IN  
THE BENEDICT-WEBB-RUBIN EQUATION OF STATE  
FOR FLUOROFORM

UNITS:  $P = \text{PSIA}$ ,  $\rho = \text{LB-MOLE/CU-FT}$ ,  $T = \text{°R}$   
 $R = 10.73185 \text{ (PSIA)(CU-FT)/(LB-MOLE)(°R)}$

$A_0 \times 10^{-1}$	-1.7492537
$B_0$	-1.0554567
$C_0 \times 10^{-10}$	1.1113494
$a \times 10^{-4}$	5.5838156
$b$	4.3249405
$c \times 10^{-10}$	2.0060423
$\alpha \times 10^{+1}$	9.6075740
$\gamma$	6.9521538

Experimental Range of Data Fitted

$T \text{ (°R)}$	852 - 1122
$P \text{ (PSIA)}$	32 - 2233
Sample Error of Estimate $\times 10^{+4}$	4.685399

TABLE 2  
 NUMERICAL VALUES OF THE CONSTANTS IN  
 THE BENEDICT-WEBB-RUBIN EQUATION OF STATE  
 FOR FLUOROFORM

UNITS:  $P = \text{ATM}$ ,  $\rho = \text{GR-MOLE/LITER}$ ,  $T = ^\circ\text{K}$   
 $R = 0.082056708 \text{ (LITER)(ATM)/(GR-MOLE)(}^\circ\text{K)}$

$A_0 \times 10^{-1}$	-4.9784139
$B_0 \times 10^{+2}$	-6.5890407
$C_0 \times 10^{-6}$	9.7562312
a	9.9208863
b $\times 10^{+2}$	1.6855548
c $\times 10^{-6}$	1.1000557
$\alpha \times 10^{+8}$	4.4926370
$\gamma \times 10^{+2}$	2.7094564

Experimental Range of Data Fitted

T ( $^\circ\text{K}$ )	473.15 - 623.15
P (ATM)	2.2 - 152
Sample Error of Estimate $\times 10^{+4}$	4.685399

TABLE 3

## HELIUM MEASUREMENT

SECOND AND THIRD VIRIAL COEFFICIENTS, APPARATUS CONSTANTS  
AND THE STANDARD ERROR OF ESTIMATE BY NON-LINEAR ANALYSIS

RUN	T°C	B <sub>2</sub> (cc/mole)	σ <sub>B<sub>2</sub></sub>	B <sub>3</sub> (cc/mole) <sup>2</sup>	σ <sub>B<sub>3</sub></sub>	N	σ <sub>N</sub>
1	200.0*	10.6 ± 0.28	0.14	106	32.7	1.408308	0.000024
2	200.0*	10.6 ± 0.26	0.13	104	24.7	1.408309	0.000023
3	250.0*	10.4 ± 0.24	0.12	99	30.7	1.408327	0.000018
4	250.0*	10.4 ± 0.42	0.21	104	41.0	1.408347	0.000044
13	300.0*	10.3 ± 0.30	0.15	99	33.4	1.403139	0.000022
14	300.0*	10.3 ± 0.28	0.14	96	37.6	1.403146	0.000019
15	350.0	10.2	0.12	99	27.9	1.402020	0.000017
16	350.0	10.3	0.10	91	23.4	1.402014	0.000013

\* The values of the second virial coefficients at these temperature has a confidential level of 95.5%

TABLE 4

AVERAGE VALUES OF THE SECOND AND THIRD VIRIAL COEFFICIENTS, APPARATUS CONSTANTS  
FROM THE HELIUM MEASUREMENTS  
AND THE STANDARD ERROR OF ESTIMATE BY NONLINEAR ANALYSIS

$T^{\circ}C$	$B_2(cc/mole)$	$\sigma_{B_2}$	$B_3(cc/mole)^2$	$\sigma_{B_3}$	N	$\sigma_N$
200.0	10.6	0.08	104	17.3	1.408308	0.000015
250.0	10.4	0.11	100	22.8	1.408335	0.000018
300.0	10.3	0.09	98	21.4	1.403142	0.000014
350.0	10.2	0.08	93	18.0	1.402016	0.000011

TABLE 5

## COMPARISON OF SECOND VIRIAL COEFFICIENTS OF HELIUM

T <sup>o</sup> C	SOURCE	B <sub>2</sub> (cc/mole)
200.0	This work	10.60
	Holborn (30,31)	11.07
	Epperly (17)	11.10
	Keesom (33)	10.59
	Schneider (48,49,65)	11.08
	Silberberg (51)	10.76
	Suh (55,56)	10.98
	Wiebe (66)	10.72
250.0	This work	10.41
	Epperly (17)	9.56
	Witonsky (67)	10.69
300.0	This work	10.31
	Epperly (17)	9.08
	Holborn (30,31)	10.50
	Keesom (33)	10.11
	Schneider (48,49,65)	10.76
	Suh (55,56)	10.59
350.0	This work	10.23
	Epperly (17)	9.40

TABLE 6

## FLUOROFORM MEASUREMENTS

SECOND AND THIRD VIRIAL COEFFICIENTS, APPARATUS CONSTANTS  
AND THE STANDARD ERROR OF ESTIMATE BY NON-LINEAR ANALYSIS

RUN	T°C	B <sub>2</sub> (cc/mole)	σ <sub>B<sub>2</sub></sub>	B <sub>3</sub> (cc/mole) <sup>2</sup>	σ <sub>B<sub>3</sub></sub>	N	σ <sub>N</sub>
5	200.0	-51.9	0.85	6504	266.6	1.408034	0.000167
6	250.0	-36.2	1.06	5333	312.8	1.405997	0.000189
7	250.0	-37.0	0.82	5348	226.5	1.405959	0.000159
8	200.0	-51.8	0.81	6502	245.3	1.408040	0.000166
9	300.0	-26.0	0.84	4488	221.1	1.403087	0.000152
10	300.0	-26.0	1.06	4495	285.9	1.403134	0.000186
11	350.0	-20.8	1.25	4162	400.8	1.401850	0.000169
12	350.0	-21.3	1.33	4266	396.9	1.401955	0.000204

TABLE 7

AVERAGE VALUES OF THE SECOND AND THIRD VIRIAL COEFFICIENTS, APPARATUS CONSTANTS  
FROM THE FLUOROFORM MEASUREMENTS  
AND THE STANDARD ERROR OF ESTIMATE BY NONLINEAR ANALYSIS

$T^{\circ}C$	$B_2(\text{cc/mole})$	$\sigma_{B_2}$	$B_3(\text{cc/mole})^2$	$\sigma_{B_3}$	N	$\sigma_N$
200.0	-51.9	0.54	6502	165.8	1.408037	0.000108
250.0	-36.0	1.14	5141	321.8	1.405905	0.000214
300.0	-26.0	0.64	4482	170.8	1.403107	0.000115
350.0	-20.9	0.83	4187	256.2	1.401889	0.000120

EXPERIMENTAL VALUES OF RUN CONSTANT AND  
 COMPRESSIBILITY FACTORS FOR FLUOROFORM AT  $T = 200^{\circ}\text{C}$

RUN 5 RUN CONSTANT = 147.69408

EXPANSION NUMBER	P (PSIA)	Z
0	1887.415406	0.8696
1	1381.557464	0.8962
2	1006.998072	0.9198
3	730.350072	0.9393
4	527.247497	0.9548
5	379.128380	0.9667
6	271.761843	0.9757
7	194.327913	0.9823
8	138.703339	0.9872
9	98.865142	0.9908
10	70.296350	0.9920
11	50.095523	0.9954
12	35.628784	0.9968

RUN 8 RUN CONSTANT = 155.50107

0	1977.729392	0.8654
1	1448.322786	0.8924
2	1056.426413	0.9165
3	766.769664	0.9366
4	553.903575	0.9527
5	398.512284	0.9651
6	285.778588	0.9745
7	204.417439	0.9815
8	145.939002	0.9688
9	104.041683	0.9904
10	73.986895	0.9917
11	52.729267	0.9951
12	37.503782	0.9966



TABLE 8 (CONTINUED)

64

EXPERIMENTAL VALUES OF RUN CONSTANT AND  
COMPRESSIBILITY FACTORS FOR FLUOROFORM AT  $T = 250^{\circ}\text{C}$ 

RUN 6 RUN CONSTANT = 142.40598

EXPANSION NUMBER	P (PSIA)	Z
0	1938.334804	0.9262
1	1397.742882	0.9390
2	1007.773548	0.9519
3	725.239028	0.9632
4	520.724902	0.9732
5	373.088604	0.9795
6	266.833455	0.9850
7	190.570594	0.9890
8	135.957126	0.9921
9	96.915445	0.9943
10	68.925013	0.9962
11	49.167993	0.9972
12	35.001665	0.9981

RUN 7 RUN CONSTANT = 157.30170

0	2127.406448	0.9203
1	1534.560720	0.9333
2	1107.503560	0.9470
3	797.883172	0.9592
4	573.457793	0.9693
5	411.209738	0.9772
6	294.290907	0.9833
7	210.285602	0.9878
8	150.077901	0.9912
9	107.010655	0.9937
10	76.142702	0.9941
11	54.307655	0.9968
12	38.666530	0.9979

TABLE 8 (CONTINUED)

EXPERIMENTAL VALUES OF RUN CONSTANT AND  
COMPRESSIBILITY FACTORS FOR FLUOROFORM AT  $T = 300^{\circ}\text{C}$

RUN 9 RUN CONSTANT = 159.07477

EXPANSION NUMBER	P (PSIA)	Z
0	2233.150750	0.9553
1	1599.153711	0.9598
2	1148.161514	0.9669
3	824.311878	0.9740
4	591.206994	0.9801
5	423.502274	0.9851
6	303.023707	0.9890
7	216.614068	0.9919
8	154.729449	0.9941
9	110.458911	0.9958
10	78.711763	0.9965
11	56.229003	0.9979
12	40.102195	0.9986

RUN 10 RUN CONSTANT = 153.38650

0	2153.956901	0.9555
1	1543.086695	0.9605
2	1107.916559	0.9676
3	795.307214	0.9746
4	570.305254	0.9806
5	408.460625	0.9855
6	292.217496	0.9893
7	208.864899	0.9921
8	149.177441	0.9943
9	106.489399	0.9959
10	75.855526	0.9971
11	54.202467	0.9979
12	38.656781	0.9987

TABLE 8 (CONTINUED)

EXPERIMENTAL VALUES OF RUN CONSTANT AND  
COMPRESSIBILITY FACTORS FOR FLUOROFORM AT  $T = 350^{\circ}\text{C}$ 

RUN 11 RUN CONSTANT = 126.09264

EXPANSION NUMBER	P (PSIA)	Z
0	1799.738038	0.9712
1	1288.758159	0.9750
2	923.789655	0.9797
3	661.987095	0.9842
4	474.038808	0.9879
5	339.185750	0.9910
6	242.527576	0.9933
7	173.315710	0.9951
8	123.800599	0.9964
9	88.401747	0.9974
10	63.008957	0.9982
11	45.043855	0.9987
12	32.147538	0.9992

RUN 12 RUN CONSTANT = 135.22785

0	1927.337761	0.9698
1	1379.545691	0.9732
2	988.847444	0.9780
3	708.701562	0.9826
4	507.575597	0.9867
5	363.241482	0.9899
6	259.764408	0.9925
7	185.654032	0.9944
8	132.633948	0.9960
9	94.706634	0.9971
10	67.505350	0.9978
11	48.261854	0.9986

**BIBLIOGRAPHY**

## BIBLIOGRAPHY

1. Anderson, L. N., Kudchadker, A. P., and Eubank, P. T., J. Chem. Eng. Data, 13, 321(1968).
2. Barker, J. A., Leonard, P. J., and Pompe, A., J. Chem. Phys., 44, 4206(1966).
3. Benedict, M., Webb, G. B., and Rubin, L. C., J. Chem. Phys., 8, 334(1940).
4. Blancett, A. L., Hall, K. R., and Canfield, F. B., Physica, 47, 75(1970).
5. Bloomer, O. T., Inst. Gas Tech. Res. Bul., 13(1952).
6. Bloomer, O. T., and Rao, K. N., Inst. Gas Tech. Res. Bul., 18(1952).
7. Briggs, T. C., and Barieau, R. E., BuMines Rept. of Inv., 7136(1968).
8. Briggs, T. C., Dalton, B. J., and Barieau, R. E., BuMines Rept. of Inv., 7287(1969).
9. Britt, H. I., and Luecke, R. H., Technometrics, 15, No. 2, 233(1973).
10. Brough, H. W., Schlinger, W. G., and Sage, B. H., Ind. Eng. Chem., 43, 2442(1951).
11. Burnett, E. S., J. Appl. Mech. A-136(1936).
12. Davison, N., "Statistical Thermodynamics," McGraw-Hill, New York, N. Y.(1962).
13. De Rocco, A. G., and Hoover, W. G., J. Chem. Phys., 36, 916(1962).
14. De Rocco A. G., Spurling, T. H., and Storvick, T. S., J. Chem. Phys., 46, 599(1967).
15. Dripps, W. E., M.S. Thesis, Dept. Ch.E., U. of Mo., Columbia, Missouri(1968).
16. Dymond, J. H., and Smith, E. B., Trans. Faraday Soc., 60, 1378(1964).
17. Epperly, A. D., Ph.D. Dissertation, Dept. Ch.E., U. of Mo., Columbia, Missouri(1970).
18. Epstein, L. F., J. Chem. Phys., 20, 1981(1952).

19. Epstein, L. F., J. Chem. Phys., 21, 762(1953).
20. Eubank, P. T., and Kerns, W. J., A. I. Ch. E. J., 19, 711(1973).
21. Hajjar, R. F., and MacWood, G. E., J. Chem. Phys., 49, 4567(1968).
22. Hajjar, R. F., and MacWood, G. E., J. Chem. Eng. Data, 15, 3(1970).
23. Hall, K. R., and Canfield, F. B., Physica, 47, 75(1970).
24. Hall, K. R., and Canfield, F. B., Physica, 47, 99(1970).
25. Hall, K. R., and Eubank, P. T., Physica, 135, 13(1972).
26. Harper, R. C. Jr., and Miller, J. G., J. Chem. Phys., 27, 36(1957).
27. Haworth, W. S., and Sutton, L. E., Trans. Farady Soc. 67, 2907(1971).
28. Hill, T. L., "Introduction to Statistical Thermodynamics," Addison-Wesley, Reading, Mass.(1960).
29. Hirschfelder, J. O., Curtiss, C. F., and Bird, R. B., "Molecular Theory of Gases and Liquids," John-Wiley and Sons, Inc., New York, N. Y.(1954).
30. Holborn L., and Otto, J., Z. Phys., 33, 1(1925).
31. Holborn, L., and Otto, J., Z. Phys., 38, 359(1926).
32. Hoover, A. E., Canfield, F. B., Kobayashi, R., and Leland, T. W. Jr., J. Chem. Eng. Data, 9, 568(1964).
33. Keesom, W. H., Helium, Table 2.14, P.49, Elsevier, Amsterdam(1942).
34. Kramer, G. M., and Miller, J. G., J. Phys., 61, 785 (1957).
35. Levelt-Sengers, J. M. H., Private Communications,(1967).
36. MacCormack, K. E., and Schneider, W. G., J. Chem. Phys., 19, 845(1951).
37. Mason, E. A., and Spurling, T. H., "The International Encyclopedia of Physical Chemistry and Chemical Physics" Topic 10, Volume 2, Pergamon Press, Oxford, England (1969).

38. Mason, E. A., And Monchick, L., "Method for determination of Intermolecular Forces," Intermolecular Forces, Interscience Publishers(1967).
39. Meyer, J. E., J. Chem. Phys., 5, 67(1937).
40. Miller, J. E., Bumines Inf. Cir., 8350(1967).
41. Mueller, W. H., Ph.D. Dissertation, Dept. Ch.E., The Rice Institute, Houston, Texas(1959).
42. Mueller, W. H., Leland, T. W., Jr., and Kobayashi, R., A. I. Ch. E. J., 7, 267(1961).
43. Onnes, K. H., Comm. Phys. Lab., 71, Leiden, Amsterdam (1901).
44. Pfefferle, W. C., Goff, J. A., and Miller, J. G., J. Chem. Phys., 23, 509(1955).
45. Pope, G. A., Chappellear, P. S., and Kobayashi, R., Physica, 57, 127(1972).
46. Putnam, W. E., and Kilpatrick, J. E., J. Chem. Phys., 21, 951(1953).
47. Ree, F. H., and Hoover, W. G., J. Chem. Phys., 46, 4181 (1967).
48. Schneider, W. G., Can. J. Research, B27, 339(1949).
49. Schneider, W. G., and Duffie, J. A. H., J. Chem. Phys., 17, 751(1949).
50. Sigmund, P. M., Silberberg, I. H., and McKetta, J. J., J. Chem. Engr. Data, 17, 168(1972).
51. Silberberg, I. H., Kobe, K. A., and McKetta, J. J., J. Chem. Eng. Data, 4, 314(1959).
52. Silberberg, I. H., McKetta, J. J., and Kobe, K. A., J. Chem. Eng. Data, 4, 323(1959).
53. Silberberg, I. H., Lin, C. N., and McKetta, J. J., J. Chem. Eng. Data, 12, 226(1967).
54. Storvick, T. S., Spurling, T. H., and De Rocco, A. G., J. Chem. Phys., 46, 1498(1967).
55. Suh, K. W., Ph.D. Dissertation, Dept. Ch.E., U. of Mo., Columbia, Missouri(1965).

56. Suh, K. W., and Storvick, T. S., A. I. Ch. E. J., 13, 231(1967).
57. Suh, K. W., and Storvick, T. S., J. Chem. Phys., 71, 1450(1967).
58. Sutter, H., and Cole, R. H., J. Chem. Phys., 46, 2014(1967).
59. Sutter, H., and Cole, R. H., J. Chem. Phys., 52, 132(1970).
60. Vogl, W. F., and Hall, K. R., Physica, 59, 529(1972).
61. Watson, G. M., Stevens, A. B., Evans, R. B. III., and Hodges, D. Jr., Ind. Eng. Chem., 46, 362(1954).
62. Waxman, M., Hastings, J. R., and Chen, T. W., Proc. Fifth Symposium, 248(ASME, New York, 1970).
63. Waxman, M., and Hastings, J. R., B. Am. Phys. S., 16, 524(1971).
64. Weast, R. C., Editor, "Handbook of Chemistry and Physics," E-70, The Chemical Rubber Co., Cleveland, Ohio (1970).
65. Whalley, E., Lupien, Y., and Schneider, W. G., Can. J. Chem., 31, 722(1953).
66. Wiebe, V. L., Gaddy, V. L., and Heins, C. Jr., J. Am. Chem. Soc., 53, 1721(1931).
67. Witonsky, R. J., and Miller, J. G., J. Am. Chem. Soc., 85, 282(1963).
68. Yntema, J. L., and Schneider, W. G., J. Chem. Phys., 18, 641 and 646(1950).
69. Zimmerman, R. H., and Beitter, S. R., Trans. A.S.M.E., 74, 945(1952).



**APPENDIXES**

## APPENDIX A

## METHOD OF NONLINEAR REGRESSION

The method of nonlinear regression based on the work of J.M.H. Levelt-Sengers (35), entitled "The Statistical Analysis of p-v-T Data and Derived Properties" is presented in this section.

A matrix is denoted by a double underline. A vector is denoted by a single underline. The transpose of a matrix is denoted by superscript "T" and the inverse is denoted by superscript "-1".

For a given set of observed values  $P_1 \dots P_m$  which are all subject to error, the expectation values of these observed quantities  $P_1 \dots P_m$  obey a set of conditions involving certain parameters  $b_1 \dots b_k$ .

$$F_1(P_1 \dots P_m, b_1 \dots b_k) = 0$$

.

.

.

$$F_n(P_1 \dots P_m, b_1 \dots b_k) = 0$$

where  $m > n > k$

(A-1)

For the case where the P's have equal variance and are not correlated,

$$\text{Var } \underline{\underline{P}} = \sigma_P^2 \times I^{m \times m} \quad (\text{A-2})$$

It is assumed here that both the observed quantities and the parameters are subject to error. The conditions  $F_1 \dots F_n$  are not linear in the coefficients  $b_1 \dots b_k$ . The coefficients  $b_j$  ( $j = 1 \dots k$ ) can be determined by requiring that the sum-of-squares of the adjustments of the observed values  $P_i$  ( $i = 1 \dots m$ ),  $SSP_i$ , to be a minimum under the constraints  $F_\ell$  ( $\ell = 1 \dots n$ ).

$$SSP_i = \sum_{i=1}^m (\Delta P_i)^2 = \min. \quad (\text{A-3})$$

$$\text{with } F_1 \dots F_n = 0, \text{ and } b_j = \tilde{b}_j$$

where  $\tilde{b}_j$  represents the values of the coefficients which will make sum-of-squares of the adjustments of the  $P_i$  ( $i = 1 \dots m$ ) a minimum under the constraints  $F_\ell$  ( $\ell = 1 \dots n$ ). Define

$$\begin{aligned} \tilde{b}_j &= b_j^o + \Delta b_j, \quad j = 1 \dots k \\ P_i &= P_i^o - \Delta P_i, \quad i = 1 \dots m \end{aligned} \quad (\text{A-4})$$

where the superscripts "o" represent the approximate value. With these approximate values the constraining equations can

be defined as,

$$\begin{aligned}
 F_1^0 &= F_1(P_1^0 \dots P_m^0, b_1^0 \dots b_k^0) \\
 &\cdot \\
 &\cdot \\
 &\cdot \\
 F_n^0 &= F_n(P_1^0 \dots P_m^0, b_1^0 \dots b_k^0)
 \end{aligned}
 \tag{A-5}$$

If the adjustments  $P_i$  ( $i = 1 \dots m$ ) are small and if the  $b_j^0$  ( $j = 1 \dots k$ ) are "good" first estimates, the constraining equations  $F_\ell^0$  ( $\ell = 1 \dots n$ ) will be close to  $F_\ell$  ( $\ell = 1 \dots n$ ). This means the differences between  $F_\ell^0$  and  $F_\ell$  are close to zero. Linearization of the constraining equations can be done by expanding the equations  $F_\ell$  ( $\ell = 1 \dots n$ ) in a Taylor's expansion with respect to  $P_i$  ( $i = 1 \dots m$ ) and  $b_j$  ( $j = 1 \dots k$ ), and retaining only the first derivatives,

$$\begin{aligned}
 F_\ell^0 &= F_\ell(P_1 \dots P_m, b_1 \dots b_k) + \sum_{i=1}^m \frac{\partial F_\ell}{\partial P_i} \\
 &\quad (P_i^0 - P_i) + \sum_{j=1}^k \frac{\partial F_\ell}{\partial b_j} (b_j^0 - \tilde{b}_j) \\
 &\quad \ell = 1 \dots n
 \end{aligned}$$

or

$$\begin{aligned}
 F_\ell^0 &= \sum_{i=1}^m \frac{\partial F_\ell}{\partial P_i} \Delta P_i - \sum_{j=1}^k \frac{\partial F_\ell}{\partial b_j} \Delta b_j \\
 &\quad \ell = 1 \dots n
 \end{aligned}
 \tag{A-6}$$

Next, define the following Jacobian matrices,

$$\underline{\underline{J}}_P^{(m \times n)} = \begin{vmatrix} \frac{\partial F_1}{\partial P_1} & \dots & \frac{\partial F_n}{\partial P_1} \\ \cdot & & \cdot \\ \cdot & & \cdot \\ \cdot & & \cdot \\ \frac{\partial F_1}{\partial P_m} & \dots & \frac{\partial F_n}{\partial P_m} \end{vmatrix} \quad (\text{A-7})$$

$$\underline{\underline{J}}_b^{(n \times k)} = \begin{vmatrix} -\frac{\partial F_1}{\partial b_1} & \dots & -\frac{\partial F_1}{\partial b_k} \\ \cdot & & \cdot \\ \cdot & & \cdot \\ \cdot & & \cdot \\ -\frac{\partial F_n}{\partial b_1} & \dots & -\frac{\partial F_n}{\partial b_k} \end{vmatrix} \quad (\text{A-8})$$

and the vectors,

$$\underline{\underline{\Delta b}}^{(k \times 1)} = \begin{vmatrix} \Delta b_1 \\ \cdot \\ \cdot \\ \cdot \\ \Delta b_k \end{vmatrix} \quad (\text{A-9})$$

$$\underline{F}^0 (n \times 1) = \begin{vmatrix} F_1^0 \\ \cdot \\ \cdot \\ \cdot \\ F_n^0 \end{vmatrix} \quad (A-10)$$

$$\underline{\Delta P} (m \times 1) = \begin{vmatrix} \Delta P_1 \\ \cdot \\ \cdot \\ \cdot \\ \Delta P_m \end{vmatrix} \quad (A-11)$$

The linearized constraining equation (A-6) can be rewritten in terms of these matrices as,

$$\underline{F}^0 = \underline{F}_P^T \underline{\Delta P} + \underline{F}_b \underline{\Delta b} \quad (A-12)$$

The matrices  $\underline{F}_P$  and  $\underline{F}_b$  are calculated approximately using the approximate value  $P^0$ ,  $b^0$ . These are substituted into the constraining equation. Because the solution involves the approximations, it may be necessary to carry the process through several iterations, in order to arrive at a satisfactory results, especially if the first estimate of the coefficients are not very good.

The variation of the sum-of-square of the differential  $\Delta P$  is required to zero under small variations of the optimum  $\Delta P$  under the constraints of the conditions.

$$\underline{P}^T \delta \Delta \underline{P} = 0 \quad (\text{A-13})$$

where

$$\underline{F}_P^T \delta \Delta \underline{P} + \underline{F}_b \delta \Delta \underline{b} = 0 \quad (\text{A-14})$$

Using the Lagrangian undetermined multiplies  $\lambda_1 \dots \lambda_n$  and equation (A-13) and (A-14),

$$(\Delta \underline{P}^T - \underline{\lambda}^T \underline{F}_P^T) \delta \Delta \underline{P} - \underline{\lambda}^T \underline{F}_b \delta \Delta \underline{b} = 0 \quad (\text{A-15})$$

where

$$\underline{\lambda}^T = \left| \lambda_1 \dots \lambda_n \right|$$

By choosing  $\underline{\lambda}^T$  appropriately, all coefficients can be made to vanish, and

$$\Delta \underline{P}^T - \underline{\lambda}^T \underline{F}_P^T = 0 \quad (\text{A-16})$$

$$\underline{\lambda}^T \underline{F}_b = 0$$

From equations (A-12) and (A-16),

$$\underline{F}^0 = \underline{F}_P^T \underline{F}_P \lambda + \underline{F}_b \Delta \tilde{b} \quad (\text{A-17})$$

Define the (nxn) matrix  $\underline{L}$  as,

$$\underline{L} = \underline{F}_P^T \underline{F}_P \quad (\text{A-18})$$

Equation (A-17) becomes,

$$\underline{F}^0 = \underline{L} \lambda + \underline{F}_b \Delta \tilde{b} \quad (\text{A-19})$$

If  $\underline{L}^{-1}$  exists and equation (A-19) is pre-multiplied by  $\underline{F}_b^T \underline{L}^{-1}$ , then,

$$\underline{F}_b^T \underline{L}^{-1} \underline{F}^0 = \underline{F}_b^T \underline{L}^{-1} \underline{F}_b \Delta \tilde{b} \quad (\text{A-20})$$

and

$$\underline{F}_b^T \underline{L}^{-1} \underline{L} \lambda = \underline{F}_b^T \lambda = 0 \quad (\text{A-21})$$

Equation (A-20) as a set of normal equations which can be solved for  $\Delta \tilde{b}$ .

$$\Delta \tilde{b} = (\underline{F}_b^T \underline{L}^{-1} \underline{F}_b)^{-1} \underline{F}_b^T \underline{L}^{-1} \underline{F}^0 \quad (\text{A-22})$$



By definition, the variance of coefficients can be written,

$$\begin{aligned}\text{Var } \underline{\underline{b}} &= E[(\underline{b} - \widetilde{\underline{b}})(\underline{b} - \widetilde{\underline{b}})^T] \\ &= (\underline{F}_b^T \underline{L}^{-1} \underline{F}_b)^{-1} \sigma_{F^0}^2\end{aligned}\quad (\text{A-23})$$

while

$$\sigma_{F^0}^2 = \frac{(\underline{F}^0 - \underline{F}_b \Delta \widetilde{\underline{b}})^T \underline{L}^{-1} (\underline{F}^0 - \underline{F}_b \Delta \widetilde{\underline{b}})}{n - k}\quad (\text{A-24})$$

$$\text{Var } \underline{F}^0 = \sigma_{F^0}^2 \underline{L}\quad (\text{A-25})$$

From equation (A-12),

$$\underline{F}^0 = \underline{F}_P^T \Delta \underline{P} + \underline{F}_b \Delta \underline{b}\quad (\text{A-26})$$

$$\underline{F}_P^T \Delta \underline{P} = \underline{F}^0 - \underline{F}_b \Delta \underline{b}$$

Substituting equation (A-26), (A-16), (A-18) into equation (A-24),

$$\begin{aligned}\sigma_{F^0}^2 &= \frac{\Delta \underline{P}^T \underline{F}_P \underline{L}^{-1} \underline{F}_P^T \Delta \underline{P}}{n - k} \\ &= \frac{\Delta \underline{P}^T \underline{F}_P \lambda}{n - k} = \frac{\Delta \underline{P}^T \Delta \underline{P}}{n - k}\end{aligned}\quad (\text{A-27})$$

From equation (A-16) and (A-19),

$$\underline{\Delta P} = \underline{F_P L}^{-1} (\underline{F^O} - \underline{F_b} \underline{\tilde{b}}) \quad (\text{A-28})$$

$\underline{\Delta P}$  can be found after calculating  $\underline{\tilde{b}}$ .

If the observed P's are varied by amount  $\delta P$ , then

$$\delta \underline{F^O} = \underline{F_P^T} \delta \underline{P} \quad (\text{A-29})$$

so that,

$$\begin{aligned} \text{Var } F^O &= E[(\delta \underline{F^O}, (\delta \underline{F^O})^T)] \\ &= E(\underline{F_P^T} \delta \underline{P}, \delta \underline{P}^T \underline{F_P}) \\ &= \underline{F_P^T} (\text{Var } \underline{P}) \underline{F_P} \\ &= \sigma_P^2 \underline{L} \end{aligned} \quad (\text{A-30})$$

where  $\text{Var } \underline{P}$  is diagonal with elements  $\sigma_P^2$ . Comparing equation (A-30) and equation (A-25), (A-27),

$$\sigma_P^2 = \frac{1}{n-k} \underline{\Delta P}^T \underline{\Delta P} \quad (\text{A-31})$$

From equation (A-23),

$$\sigma_b^2 = (\underline{F_b^T L}^{-1} \underline{F_b})^{-1} \sigma_P^2 \quad (\text{A-32})$$

For the case in which P's are correlated and of unequal variance,

$$\text{Var}\underline{\underline{P}} = \sigma_P^2 \underline{\underline{A}}^{(m \times m)} \quad (\text{A-33})$$

Equation (A-33) can be converted to the same form as equation (A-2). Defining a matrix  $\underline{\underline{R}}$ ,

$$\underline{\underline{R}}\underline{\underline{R}}^T = \underline{\underline{A}}^{-1} \quad \text{or} \quad \underline{\underline{R}}^T \underline{\underline{A}} \underline{\underline{R}} = \underline{\underline{I}}^{m \times m} \quad (\text{A-34})$$

$$\underline{\underline{\tilde{P}}} = \underline{\underline{R}}^T \underline{\underline{P}} \quad (\text{A-35})$$

$$\text{Var}\underline{\underline{\tilde{P}}} = \underline{\underline{R}}^T \text{Var}\underline{\underline{P}} \underline{\underline{R}} = \sigma_P^2 \underline{\underline{R}}^T \underline{\underline{A}} \underline{\underline{R}} = \sigma_P^2 \underline{\underline{I}}^{m \times m} \quad (\text{A-36})$$

Equation (A-36) has the similar form as equation (A-2).

By following the same procedure as indicated from equation (A-3) to equation (A-32). The final results are:

$$\underline{\underline{L}} = \underline{\underline{F}}_P^T \underline{\underline{A}} \underline{\underline{F}}_P \quad (\text{A-37})$$

$$\Delta \underline{\underline{b}} = (\underline{\underline{F}}_b^T \underline{\underline{L}}^{-1} \underline{\underline{F}}_b)^{-1} \underline{\underline{F}}_b^{-1} \underline{\underline{L}} \underline{\underline{F}}_b^0 \quad (\text{A-38})$$

$$\Delta \underline{\underline{\tilde{P}}} = \underline{\underline{A}} \underline{\underline{F}}_P \underline{\underline{L}}^{-1} (\underline{\underline{F}}_b^0 - \underline{\underline{F}}_b \Delta \underline{\underline{b}}) \quad (\text{A-39})$$

$$\sigma_{\tilde{P}}^2 = (\Delta \underline{\underline{P}}^T \underline{\underline{A}}^{-1} \Delta \underline{\underline{P}}) / (n - k) \quad (\text{A-40})$$

$$\sigma_b^2 = (\underline{F}_b^T \underline{L}^{-1} \underline{F}_b)^{-1} \sigma_P^2 \quad (\text{A-41})$$

The matrix  $\underline{A}$  is a diagonal with elements  $1/w_1 \dots 1/w_m$ ,

$$A = \begin{vmatrix} 1/w_1 & & & & \\ & \cdot & & & \\ & & \cdot & & \\ & & & \cdot & \\ & & & & 1/w_m \end{vmatrix} \quad (\text{A-42})$$

where  $w$ 's are commonly denoted as the weights of the measurements  $P_1 \dots P_m$ , and equal to  $(P_i + 3)^2$ ,  $i = 1 \dots m$ .

## APPENDIX B

## DESCRIPTION OF THE MEASURING INSTRUMENTS

Detailed descriptions of the various instruments are included in the instruction manuals supplied by the manufacturers. Only a brief summary is presented here.

A. Pressure Measuring Instruments

The pressure measuring instruments were done on two instruments. One was a Ruska Model 2400 oil lubricated Dead Weight Gauge (DWG) with two Ruska Differential Pressure Indicators (DPI). The oil lubricated Dead Weight Gauge was used for measuring the system gas pressure. The other gauge was a Ruska Model 2465 Air Piston Gauge with one Ruska Model 2416 control box. This gauge was used to measure the atmospheric pressure and this was used to convert the system gas pressure to absolute pressure.

Oil Lubricated Dead Weight Gauge and Differential Pressure Indicator

The piston of the Ruska Model 2400 Dead Weight Gauge was made of tungsten carbide, and has an enlarged section on its lower end for the purpose of over pressure

protection. The cylinder is of the re-entrant type which permits high operating pressure without excessive oil flow, and was made of A.I.S.I. type D2 steel. The tolerance of the piston diameter and the roundness was of the order of  $5 \times 10^{-6}$  in. A circular table was mounted on the piston and the weights were placed on this when the gauge was in use. The combined mass of the weight table assembly and the piston constituted the tare weight of the piston. The tare weight divided by the piston area represents the minimum pressure which the gauge can measure.

During the operation of the Dead Weight Gauge, the piston was rotated either clockwise or counterclockwise by means of a pulley and an electric motor arrangement. The rotation of the piston provides the alignment of the piston in the cylinder due to the viscous force in the annulus, and eliminates the friction by preventing the direct contact of the piston and the cylinder. The counter rotation eliminates the screw effect of machining or polishing marks on the piston and the cylinder.

All weights used on the Dead Weight Gauge were made of type 303 stainless steel and were calibrated in English units, and dynamically balanced for rotation. The calibration of the weights was made and reported to a precision of one part in fifty thousand for weights greater than 0.1 pound mass, one part in twenty thousand for weights 0.01 to 0.1 pound mass and one part in ten thousand for weights 0.001 to 0.01 pound mass. The calibration report for the

weights is given in Table E-2. The constants and parameters necessary for the proper conversion of the gauge loading to pressure were obtained from the test report and are summarized below:

(i) High-Range Dead Weight Gauge

Manufacturer: Ruska Instruments Corporation

Model: 2400H

Serial number: 10210 gauge

Calibration job number: A3535/C2516

Cylinder number: HC-156

Range: 30 to 12,140 psi

$A_0$ : 0.0260411 in<sup>2</sup>

Reference temperature: 25°C

$b$ :  $-3.6 \times 10^{-8}$ /psi

Thermal coefficient (C):  $1.7 \times 10^{-5}$ /°C

Resolution\*: less than 5 ppm

Leak rate: 0.02 in/min

Plane of reference: 0.03 in. below line on sleeve  
weight

(ii) Low-Range Dead Weight Gauge

Manufacturer: Ruska Instruments Corporation

Model: 2400L

Serial number: 10211 gauge

Calibration job number: A3535/C2516

Cylinder number: LC-147

Range: 6 to 2,428 psi

$A_0$ : 0.130222 in<sup>2</sup>

Reference temperature: 25°C

$b$ :  $-4.8 \times 10^{-8}$ /psi

Thermal coefficient (C):  $1.7 \times 10^{-5}$ /°C

Resolution\*: less than 5 ppm

Plane of reference: at the line on the sleeve weight

\* The resolution is designated as the smallest change in the mass of the test gauge load that will produce a measurable change in the condition of equilibrium of the two gauges and expressed as the ratio of change in mass to the total mass.

The Differential Pressure Indicator, composed of Differential Pressure Cell and Electronic Null Indicator was capable of detecting any instantaneous pressure differentials in both low and high pressure system. A thin stainless steel diaphragm separates the two pressure chambers of the Differential Pressure Cell. The diaphragm assembly positions an iron core inside a linear differential transformer coil located in the upper pressure chamber. The deflection of the diaphragm caused by different pressures across the diaphragm change the relative position of the core and coil. This change of the core-coil relationship causes an electrical output which was detected on a bridge circuit. A calibration curve for the zero shift as a function of operating pressure was supplied with each unit



by Ruska Instruments Corporation.

(i) Low Temperature Differential Pressure Indicator

Manufacturer: Ruska Instruments Corporation

Model: 2416.1

Cell serial number: 10132

Cell catalog number: 2413

Electronic Null Indicator serial number: 10322

Electronic Null Indicator catalog number: 2416

Sensitivity:  $1 \times 10^{-4}$  psi/micro amp

Maximum operating pressure: 15,000 psi

Maximum over-pressure on either side of diaphragm:  
15,000 psi

Temperature range: 40°F to 130°F

Zero shift:  $P_l = P_u + (0.229 \times 10^{-4}) \times P_u$

Accuracy: The accuracy of the null point is  $\pm 1\frac{1}{2}$

scale divisions under the worst case of

combined operating conditions of 10% line

voltage variation, 20°C to 40°C temperature

variation and over a period of 2 hours

continuous operation. This corresponds

to a  $3 \times 10^{-4}$  psi variation.

(ii) High Temperature Differential Pressure Indicator

Manufacturer: Ruska Instruments Corporation

Model: 216R

Cell serial number: 13221

Cell catalog number: 216R

Electronic Null Indicator serial number: 13153

Electronic Null Indicator catalog number: 2416

Sensitivity:  $2.0 \times 10^{-4}$  psi/micro amp

Maximum operating pressure: 10,000 psi

Maximum over-pressure on either side of diaphragm:  
10,000 psi

Temperature range: 40°F to 130°F

Zero shift:  $P_l = P_u + (0.515 \times 10^{-4}) \times P_u$

### Air Piston Gauge

The Air Piston Gauge was an air lubricated Dead Weight Gauge for precise measurement of gas pressure. The design basis is the same as the oil lubricated Dead Weight Gauge. The piston was lubricated by the air as the pressure transmitting medium and rotated at a constant velocity to insure consistent pressure reading. The minimum pressure at which the gauge can perform is thus limited by the lubricating film and is of the order of four tenths of a psia. The low range Air Piston Gauge was equipped with a bell jar, remote weight loader and a special set of weights for atmospheric and sub-atmospheric pressure measurements. The pressure control pack connected to both the high pressure range and the low pressure range Air Piston Gauges served as pressure adjusting device. Two pressure gauges allow the operator to monitor the pressure at the outlet of the control pack. The fine adjustment of outlet pressure

was controlled by a hand pump on the control pack. The specifications for each gauge supplied by the manufacturer are listed as follows:

(i) High Pressure Range Air Piston Gauge

Manufacturer: Ruska Instruments Corporation

Model: 2465

Serial number: 14672

Calibration job number: A7377/C7739

Cylinder and Piston number: V-281

Normal range: 2 to 600 psi

Increments: 0.5 psi

Effective area ( $A_e$ ) at 20°C: 0.013003 in<sup>2</sup>

Thermal coefficient of superficial expansion:  $9.1 \times 10^{-6}/^{\circ}\text{C}$

Piston material: tungsten carbide

Cylinder material: tungsten carbide

Piston tare: 0.0260145 pound

Piston density: 10.16 gm/cm<sup>3</sup>

Resolution:  $1 \times 10^{-4}$  psi at 2 psi

$5 \times 10^{-3}$  psi at 600 psi

Humidity range: 0 - 80% relative

Temperature range: 60 - 100°F

Reference pressure: atmospheric or vacuum

Recommended pressure medium: dry, clean nitrogen

Sink rate: maximum 0.046 in/min

Estimate system error in  $A_e$ : 62 ppm

Random error of comparison (standard deviation):

1.5 ppm

NBS reference test number for reported value of

$A_e$ : P7036B

NBS reference test number for reported values of

mass: 2.6/167716, set B; 178648, set A

Pressure gauge weights from Ruska Instruments Corp.

with catalog number 2460-910, serial number 14977

are listed in Table E-2. Deviation from the true

value of the mass will not exceed 10 ppm or 0.001

gram whichever is greater.

(ii) Low Pressure Range Air Piston Gauge

Manufacturer: Ruska Instruments Corporation

Model: 2465

Serial number: 14024

Calibration job number: C6556/A6489

Normal range: 0.2 - 15 psig

Increments: 0.0125 psig

Effective area ( $A_e$ ) at 20°C: 0.520372 in<sup>2</sup>

Thermal coefficient of superficial expansion:

$$-2.0 \times 10^{-5} / ^\circ\text{C}$$

Piston material: tungsten carbide

Cylinder material: tungsten carbide

Piston tare: 0.104056 pound

Piston density: 10.16 gm/cm<sup>3</sup>

Resolution:  $1 \times 10^{-6}$  psi at 0.2 psi

$3 \times 10^{-4}$  psi at 15 psi

Humidity range: 0 - 80% relative

Temperature range: 60 - 100°F

Reference pressure : vacuum

Recommended pressure medium: dry, clean nitrogen

(iii) Pressure Control Pack

Manufacturer: Ruska Instruments Corporation

Model: 2461

Serial number: 14021

Catalog number: 2461.1

Inlet pressure to pack: vacuum to 1,000 psi

Outlet pressure from control pack: vacuum to 1,000 psi

B. Temperature Measurement and Control Equipment

(a) Temperature Measurement Equipment

The platinum resistance thermometer, Mueller Bridge, and the optical Galvonmeter comprised the temperature measurement devices, and are discussed in that order.

Platinum Resistance Thermometer

The platinum resistance thermometer, manufactured by Rosemont Engineering Co. was designed for the range from -183°C to 500°C. The annealed high purity platinum wire resistor was hermetically sealed in a close fitting type

321 stainless steel well. The sensitive portion was at the lower two inches of the well. The thermometer had two current and two potential leads. The current to the resistance is maintained at approximately 0.5 milliamps to keep the self-heating of the thermometer in the range significantly below one thousandth of a degree C. The measured resistance between the lead junctions can be converted to temperature reading by the following equation,

$$\frac{R_t}{R_0} = 1 + \alpha \left( t - \delta \left( \frac{t}{100} - 1 \right) \left( \frac{t}{100} \right) - \beta \left( \frac{t}{100} - 1 \right) \left( \frac{t}{100} \right)^3 \right) \quad (B-1)$$

where  $\beta$  is defined as zero when  $t$  is greater than  $0^\circ\text{C}$  and  $\alpha = 0.0039257_{62}$ ,  $\delta = 1.491_{57}$ ,  $\beta = 0.110_{42}$ ,  $R_0 = 25.550$  abs. ohm.

The thermometer was calibrated by the National Bureau of Standards and certified at  $-183^\circ\text{C}$ ,  $0.001^\circ\text{C}$ ,  $100^\circ\text{C}$  and  $250^\circ\text{C}$  with the triple point of water as reference point.

### Specifications

Manufacturer: Rosemont Engineering Company

Model: 162C

Serial number: 49

NBS calibration test number: 3.1/31709

Temperature range:  $-200^\circ\text{C}$  to  $500^\circ\text{C}$

Stability: better than  $0.01^{\circ}\text{C}$

Insulation resistance: greater than 5,000 megohms at  
100V. DC at room temperature

Pressure range: 0 to 2,000 psi

### Mueller Bridge

This bridge was designed for the accurate measurement of temperature with a resistance thermometer. It had a one to one ratio and was made of two ratio arms of 1,000 ohms each. The rheostat arm of 141.1110 ohms was controlled by one plug switch and five dial switches. There was also a reversing mercury commutator that was used to eliminate the effect of possible inequalities in the thermometers lead resistance. There was a calibration arrangement for checking the bridge zero and the equality of the ratio arms. It had terminal binding posts for connecting the resistance thermometer, a battery and the galvanometer. There were two push-button controlled keys for closing the circuit between the battery and the bridge. One of the keys placed a 10,000 ohms resistor in series with the battery to decrease the sensitivity of the galvanometer for readings that were substantially away from the null resistance setting of the potentialmeter. The overall limit of error of the bridge is 0.02% of its setting or 0.00005 ohm whichever is greater.

### Specifications

Manufacturer: Minneapolis-Honeywell Regulator Co.,  
Rubicon Instruments

Catalog number: 1551

Serial number: 125202

### Galvanometer

A reflecting high sensitivity galvanometer equipped with focusing mirror for use with a lamp and scale at 1 meter distance is used to balance the bridge. A damping key is provided in the galvanometer circuit to reduce the oscillations of the moving coil.

### Specifications

Manufacturer: Minneapolis-Honeywell Regulator Co.,  
Rubicon Instruments

Catalog number: 3201, type T

Serial number: 120375

Resistance: 11.5 ohms

Sensitivity per mm at 1 meter distance: 0.071 microvolt

Period: 10 seconds

Ext. Crit. Damp. resistance: 17 ohms

Cat. No. for lamp and scale reading device: 3910

Cat. No. for right angle prism: 3280

Cat. No. for galvanometer bracket: 3290



(b) Temperature Control Equipment

A general purpose laboratory temperature controller with a platinum resistance thermometer bulb temperature sensing element and two Cenco stainless steel strip heaters were used to control the bath temperature. This temperature controller was designed to control the temperature by any one of the three modes: on-off, proportional, or proportional with reset.

For on-off operation, wheatstone bridge with a resistance thermometer detector as the variable arm, was operated at balance using an adjustable ratio arm to select the temperature setting. The temperature difference between "on" and "off" operation was  $0.001^{\circ}\text{C}$ . With proportional control, a negative feedback signal was applied to produce an "on" period which is a function of the bridge unbalance voltage. The sensitivity of the proportional controller, expressed as the proportional band temperature differential, 0 - 100% duty cycle, could be adjusted in nine steps from  $0.023^{\circ}\text{C}$  to  $5.888^{\circ}\text{C}$  with the gain switch. For reset operation, a positive feedback circuit with an adjustable time constant was added to the negative feedback circuit to eliminate the characteristic off-set of the proportional control. When the controller was used in proportional and reset mode to regulate the temperature of the bath, this reduced the apparent proportional band by a factor of 100. The reset rate for the temperature controller could be

adjusted from 6 to 90 seconds in eight steps.

### Specifications

#### Temperature Controller

Manufacturer: Hallikainen Instruments Co.

Model: Thermotrol 1053A

Serial number: 8379

#### Platinum Resistance Thermometer Bulb

Manufacturer: Hallikainen Instruments Co.

Model: 11830

Serial number: 8031

The room temperature could be controlled within  $\pm 0.1^{\circ}\text{C}$  by using the combination of a Versa-Thermo electronic controller (made by Cole-Parmer Instrument and Equipment Co.), a model 50GA006500 Carrier Air Conditioner and a Kenmore room electrical heater.

#### (c) Gas Samples

The fluoroform or Freon-23 gas was donated by E.I. du Pont de Nemours and Company. It had a specified purity of 99.9899%. The principle impurity was tetrafluoromethane.

The purity of helium was 99.995% and the purity of nitrogen was 99.997%. The helium and the nitrogen gases were purchased from the Matheson Co. Inc.

## APPENDIX C

## CORRECTIONS FOR PRESSURE MEASUREMENTS

The true pressure measurements of the Burnett cell were obtained by applying the corrections described below to the readings of both the oil lubricated and the air lubricated Dead Weight Gauges, hydraulic head corrections were also applied due to the difference in elevation between the Burnett cell and the Dead Weight Gauges. The discussion of these corrections were given in the gauge manufacturers literature and the test reports for the gauges.

(A) Corrections for the Oil Lubricated Dead Weight Gauge(i) Temperature

The effective area of the oil lubricated DWG was temperature sensitive and had to be corrected to a reference temperature. The mean of the areas of the cylinder and the piston with the piston concentric to the cylinder and falling at such a rate that the volume displaced by the piston is equal to the volumetric leakage between them provides the area of the DWG piston-cylinder system. The fractional change in effective piston area due to the variation of the

ambient temperature could be obtained by a straightforward application of the thermal expansion coefficients of the materials of the piston and the cylinder. The thermal expansion coefficients  $C_o$  was given in the test report information in the Appendix B. The relationship between the effective piston area and the ambient temperature was represented by the following linear equation,

$$A_o(t + \delta t) = A_{(t=25^{\circ}C)} \times (1 + C_o \delta t) \quad (C-1)$$

(ii) Elastic Distortion

In the piston gauge, there exists a pressure gradient along the length of the annulus between the piston and the cylinder. For high pressure measurements, the largest pressure gradient was at the bottom of the piston gauge with the total pressure equal to the pressure being measured. The stress in the piston-cylinder caused by the pressure drop through the annulus produced an elastic strain in the cylinder in the direction of the bore. Consequently, the bore in the cylinder was reduced in diameter and the area of the annulus around the piston was increased. The changes of the effective area of the piston gauge due to the pressure changes were represented by the following equation,

$$A_e = A_o(1 + B_o P) \quad (C-2)$$

The constant  $B_0$  was also given in the gauge test results. The correction introduced at 3,000 psi was less than 0.011% with an estimated accuracy of about 0.001%.

(iii) Gravitation Force

Values of the weights for the Dead Weight Gauge were reported as "pound apparent mass vs. brass standard" which is proportional to the local acceleration due to gravity. The correction of the gauge reading for any location other than the standard value of the calibration was expressed by the following equation,

$$W = M \times (g_1/g_s) \quad (C-3)$$

The standard value of gravity was chosen as 980.665 gm/sec<sup>2</sup>. The local value of gravity for Columbia, Missouri was calculated as 980.016 gm/sec<sup>2</sup> (55). The estimated correction was about 0.001%.

(iv) Buoyancy

The reported mass values for the weights shown in Table E-2 were those which the weights appear to have when compared in free air under normal conditions against normal brass standards. Since the air does have a buoyant effect on the masses it reduces the value of masses by an amount equal to the mass of air occupied by the weights. An

appropriate correction was made using the following relation,

$$W = M_a (1 - \text{density of air/density of brass}) \quad (\text{C-4})$$

The density of brass was 8.4 gm/cc and the density of air was about 0.0012 gm/cc. The approximation in equation (C-4) is good to about 1 ppm.

The corrections to the pressure for the oil lubricated Dead Weight Gauge can be combined to give the expression,

$$P = W/A$$

$$= \frac{M_a (g_1/g_s) (1 - \rho_{\text{air}}/\rho_{\text{brass}})}{A_o (25^\circ\text{C}) (1 + C_o \delta t) (1 + B_o P)} \quad (\text{C-5})$$

The maximum correction was about 0.01% for the measurements reported in this work.

(B) Correction for the Air Lubricated Dead Weight Gauge

The pressure corrections for the air lubricated Dead Weight Gauge included the variation of the acceleration of gravity, temperature, air buoyancy, and these can be expressed as,

$$P_{\text{corrected}} = P_{\text{nominal}} (1 + F_1 + F_2 + F_3) \quad (\text{C-6})$$

The factor  $F_1$  corrected for the variation of effective areas from a nominal value due to the local acceleration of gravity.

$$F_1 = (g_{\text{local}}/g_{\text{standard}})(A_o/A_e) - 1 \quad (\text{C-7})$$

The factor  $F_2$  corrected for the variation of effective areas from a nominal value due to the variation of temperature.

$$F_2 = C_o \times (t_{20^\circ\text{C}} - t_{\text{gauge}}) \quad (\text{C-8})$$

Where  $C_o$  was equal to  $2.0 \times 10^{-5}$  for low pressure range piston and  $1.0 \times 10^{-5}$  for high pressure range piston.

The factor  $F_3$  corrected for the variation of air buoyancy.

$$F_3 = -(P_{\text{ref}} \times 10^{-5}) \quad (\text{C-9})$$

The maximum correction to the air lubricated Dead Weight Gauge measurements was about 0.002%.

(C) Correction for the Differential Pressure Indicator  
Zero Shift

A differential pressure across the diaphragm causes the diaphragm to deflect. The change in pressure in a

series of Burnett cell expansions changes the null pressure position of the core in the linear differential transformer. This change in position is the zero shift. The zero shift calibration curve for each unit was supplied by the manufacturer. The estimated error magnitude of these calibration curves was about 0.002%.

(D) Corrections for the Hydraulic Head

In order to achieve the precise pressure measurements using the Dead Weight Gauge, it was necessary to consider the pressure gradient throughout the hydraulic system that results from the different densities of the pressure transfer fluid and the relative position of each gauge with respect to the Burnett cell. The pressure exerted by a hydraulic head can be found by using the following relation,

$$P = \delta H \times (g_1/g_c) \quad (C-10)$$

Figure 1 shows the vertical dimensions of the system. Since the reference plane of the low temperature Differential Pressure Cell and the two oil lubricated Dead Weight Gauges coincided, the hydraulic head corrections in the oil system can be ignored entirely. The pressure exerted at the diaphragm of the high temperature Differential Pressure Cell by the hydraulic heads can be calculated by using the following equation,



$$P_h = [\rho_A(H_2 - H_1) + \rho_R(H_0 - H_2)] \times g_1/g_c \quad (C-11)$$

where  $H_0 = 0$  (reference plane)

$$H_1 = 16\frac{1}{2} \text{ in.}$$

$$H_2 = 37\frac{3}{4} \text{ in.}$$

Subscript A: property at average temperature set equal to arithmetical mean of the bath temperature plus room temperature.

Subscript R: property at room temperature.

$\rho$ : density of nitrogen gas.

The density of nitrogen gas was determined using the Benedict-Webb-Rubin equation of state (6).

$$P = RTP + (B_0RT - A_0 - C_0/T^2)\rho^2 + (bRT - a)\rho^3 + c/T^2(1 + \gamma\rho^2)(\exp(-\gamma\rho^2))^3 + \alpha\rho^6 \quad (C-12)$$

$$\text{where } A_0 = 1.19257 \quad a = 0.149013 \quad \alpha = 0.000291569$$

$$B_0 = 0.0458013 \quad b = 0.00198165 \quad \gamma = 0.00750042$$

$$C_0 = 5889.0 \quad c = 548.110$$

$$R = 0.0820567 \text{ liter-atm/(gram-mole)}^{-\circ\text{K}}$$

It was also necessary to determine the hydraulic pressure relating to the zero reading of the Differential Pressure Indicator at each temperature to the negative of equation (C-11) evaluated at the atmospheric pressure,

$$P_h = (\delta\rho_A(H_2 - H_1) + \delta\rho_R(H_0 - H_2)) \times g_1/g_c \quad (C-13)$$

where  $\delta\rho_A = \rho_P(T_A) - \rho_{P_0}(T_A)$

$$\delta\rho_R = \rho_P(T_R) - \rho_{P_0}(T_R)$$

$P_0$  = the barometric pressure when the DP cell were zeroed.

The order of magnitude of the hydraulic head correction was 0.007% while that of zero correction varies from 0.007% at low pressure to about  $4 \times 10^{-4}\%$  at 2,000 psi. The uncertainty of the combination of zero correction and the hydraulic head correction was about 0.015% at 20 psi and decreases rapidly as the pressure increases.

The barometric pressure reading from the mercury barometric can be read within an accuracy of  $\pm 0.2$  mm Hg. This uncertainty introduced an error of 0.02% or less at 20 psi and decreases rapidly as the pressure increases.

By combining the corrections described above, the final corrected pressure reading equals to corrected gauge pressure plus hydraulic head correction plus zero correction plus zero shift correction and plus barometric pressure. The total possible uncertainty introduced to all pressure measurements were less than 0.049%.

## APPENDIX D

COMPUTER PROGRAM USED TO EVALUATE  
THE APPARATUS CONSTANT,  
THE SECOND AND THE THIRD VIRIAL COEFFICIENTS  
FROM BURNETT P-V-T MEASUREMENTS

The program for computing the virial coefficients of the virial equation of state from experimental data obtained by the Burnett method was based on the algorithm developed by Britt and Luecke (9).

The approach differs from the regression analysis of J.M.H. Levelt-Senger's work (35) in that the virial coefficients are found that fit the "corrected" experimental data exactly while minimizing the sum-of-squares of the error in the experimental pressure measurements.

The true maximum likelihood estimates for the measured pressure,  $p$ , and the virial coefficients,  $b$ , requires an iterative solution of the following equations,

$$\underline{b} - \underline{b}_i = (\underline{F}_b^T \underline{L}^{-1} \underline{F}_b)^{-1} \underline{F}_b^T \underline{L}(\underline{F}(p_i, b_i) - \underline{F}_p(p_m - p_i)) \quad (D-1)$$

$$p - p_i = (p_m - p_i) + \underline{A} \underline{F}_p \underline{L}^{-1}(\underline{F}(p_i, b_i) - \underline{F}_b(\underline{b} - \underline{b}_i) - \underline{F}_p(p_m - p_i)) \quad (D-2)$$

where the subscripts "i" represent the latest estimate of the true value, the subscripts "m" represent the experimental observed value.

The equation (D-1) and (D-2) differ from the equations (A-38) and (A-39) in Appendix A by allowing both the measured pressures and the virial coefficients to be simultaneously

adjusted to their "true" values. The iterations are continued until a  $\Delta b$  is obtained that minimizes the sum-of-squares of the error in the experimental pressure measurements.

The detailed development of algorithm can be found in the paper by Britt and Luecke (9).

```

IMPLICIT REAL*8 (A-H,O-Z)
DOUBLE PRECISION L,LI
INTEGER P,PD
DIMENSION B(12)
DIMENSION X(3,1),Z(13,1),ZI(13,1),ZPRIM(13,1),ZIZ(13,1),ADF(12,1),
$F(12,1),FZ(13,12),FX(12,3),FXT(3,12),FZI(13,12),R(13,13),DA(12,1),
$DR(13,12),L(12,12),LI(12,12),CC(3,12),Q(3,3),PI(3,3),OD(3,12),
$DELX(3,1),DF(12,1),RADF(12,1),DF(13,12),DELZ(13,1)
DIMENSION RI(13,13),DELZI(1,13),DELZTR(1,13),SIGMA2(1,1),
$PISIG(3,3)
DIMENSION FLAM(12,1),FZTLAM(13,1),FXTLAM(3,1)
DIMENSION FZDELZ(12,1)
DIMENSION CS(3,3),PIS(3,3)
DIMENSION FT(1,12)
COMMON KD,ND,PD
C CALCULATION OF SECOND AND THIRD VIRIAL COEFFICIENTS FROM
C PRESSURE MESUREMENTS OF BURNETT APPARATUS
AA=0.00
SS=1.00
IS=5
T=623.1500
PRINT 41,T
41 FORMAT(1CX,' T= ',F12.6)
RT=T*82.056700
12 CALL READ(X,Z,R,K,N,P,ITER)
PC=P
ND=N
KC=K
DC 2 I=1,P
2 ZI(I,1)=Z(I,1)
DC10 JJ=1,ITER
CALL FUNC(X,ZI,F,FX,FZ)
DC 4 I=1,P

```

```

4 ZIZ(I,I)=ZI(I,I)-Z(I,I)
  CALL MULT(FZ,ZIZ,DA,K,P,P,I)
  DC 5 I=1,K
5 ADF(I,I) = F(I,I) - DA(I,I)
  CALL TRANS(FZ,FZI,K,P)
  CALL TRANS(FX,FXI,K,N)
  CALL MULT(R,FZI,CS,P,P,P,K)
  CALL MULT(FZ,OB,L,K,P,P,K)
  CALL INVERT(L,LI,K)
  CALL MULT(FXT,LI,DC,N,K,K,K)
  CALL MULT(DC,FX,Q,N,K,K,N)
  DO 30 I=1,N
  DO 30 J=1,N
30 QS(I,J)=Q(I,J)/DSQRT(C(I,I)*C(J,J)).
  DO 32 I=1,N
32 QS(I,I)=CS(I,I)+AA
  CALL INVET2(QS,PIS,N)
  DC 31 I=1,N
  DC 31 J=1,N
31 PI(I,J)=PIS(I,J)/DSQRT(Q(I,I)*Q(J,J))
  CALL MULT(PI,DC,DC,N,N,K)
  CALL MULT(CD,ACF,DELX,N,K,K,I)
  CALL MULT(FX,DELX,DE,K,N,N,I)

```

```

DO 6 I=1,K
6 RADF(I,1)=ADF(I,1)+DE(I,1)
  CALL MULT(DB,LI,DF,P,K,K,K)
  CALL MULT(CF,RADF,DELZ,P,K,K,1)
  CALL MULT(LI,RADF,RLAM,K,K,K,1)
  CALL MULT(FZT,RLAM,FZTLAM,P,K,K,1)
  CALL MULT(FXT,RLAM,FXTLAM,N,K,K,1)
  CALL MULT(FZ,DELZ,FZDELZ,K,P,P,1)
DC 7 I=1,P
  IF(JJ.GE.IS) ZI(I,1)=Z(I,1)-DELZ(I,1)
7 CONTINUE
DC 8 I=1,N
  X(I,1)=X(I,1)-DELX(I,1)*SS
  PRINT 25,JJ
25 FCRMAT(///I5//)
  B(1)=RT*X(2,1)
  B(2)=RT**2*(X(3,1)+X(2,1)**2)
  PRINT 101,B
101 FCRMAT(//3F20.7//)
10 PRINT 11,(X(I,1),I=1,N)
11 FCRMAT(//3(1P20.7)//)
  PRINT 151,(Z(I,1),I=1,P)
  PRINT 151,(DELZ(I,1),I=1,P)
151 FCRMAT(//5(1P20.7)//)
  PRINT 21,(F(I,1),I=1,K)
21 FCRMAT(//4D20.5//)
  CALL INVET3(R,RI,P)
  CALL TRANS(DELZ,DELZT,P,1)
  CALL MULT(DELZT,RI,DELZTR,1,P,P,P)
  CALL MULT(DELZTR,DELZ,SIGMA2,1,P,P,1)
  PRINT 102,SIGMA2
  SIGMA2(1,1)=SIGMA2(1,1)/(K-N)
  PRINT 102,SIGMA2

```



```
102 FORMAT(/C20.5/)
   DO 19 I=1,N
   DO 19 J=1,N
19  PISIG(I,J)=PI(I,J)*SIGMA2(1,1)
      VB1=RT**2*PISIG(2,2)
      SDB1=DSQRT(VB1)
      SDVK=DSQRT(PISIG(1,1))
      VR2=RT**4*PISIG(3,3)+4.00*RT**4*X(2,1)**2*PISIG(2,2)
      $+4.00*RT**4*X(2,1)*PISIG(3,2)
      SDB2=DSQRT(VB2)
   PRINT 131,SDVR,SDB1,SCB2
131  FCRMAT(/F30.10//)
      CALL SKIP
      STOP
      END
```

```

SUBROUTINE MATINC (A,N,B,M,DETERM,KC,PIVOT,IPIVOT,INDEX)
IMPLICIT REAL*8 (A-H,O-Z)
DIMENSION IPIVOT(N), A(N,N), B(N,1), INDEX(N,2), PIVOT(N)
EQUIVALENCE (IRCW,JRCW), (ICCLUM,JCCLUM), (AMAX, T, SWAP)
ABS(X)=DABS(X)
SQRT(X)=DCSQRT(X)
FLOAT(N)=DFLOAT(N)
KC=1
DEL=0.
DO 902 J=1,N
DO 902 K=1,N
902 DEL=DEL+(A(J,K)*A(J,K))
DEL=(SQRT(DEL)/FLCAT(N))*1.0E-10
DETERM=1.0
DO 20 J=1,N
20 IPIVOT(J)=0
DO 550 I=1,N
AMAX=0.0
DO 105 J=1,N
IF (IPIVOT(J)-1) 60, 105, 60
60 DO 100 K=1,N
IF (IPIVOT(K)-1)80,100,901
80 IF (ABS(AMAX)-ABS(A(J,K))) 85,100,100
85 IROW=J
ICCLUM=K
AMAX=A(J,K)
100 CCNTINUE
105 CCNTINUE
IPIVOT(ICOLUM)=IPIVOT(ICOLUM)+1
IF (IRCW-ICCLUM) 140, 260, 140
140 DETERM=-DETERM
DO 200 L=1,N
SWAP=A(IRCW,L)

```

MATIN003

MATIN004  
MATIN005  
MATIN006  
MATIN007  
MATIN008  
MATIN009  
MATIN010  
MATIN011  
MATIN012  
MATIN013  
MATIN014  
MATIN015  
MATIN016  
MATIN017  
MATIN018  
MATIN019  
MATIN020  
MATIN021  
MATIN022  
MATIN023  
MATIN024  
MATIN025  
MATIN026  
MATIN027  
MATIN028  
MATIN029

```

A(IROW,L)=A(ICCOLUM,L)
200 A(ICCOLUM,L)=SWAP
    IF(M) 260, 260, 210
210 DC 250 L=1, M
    SWAP=B(IROW,L)
    B(IROW,L)=B(ICCOLUM,L)
250 B(ICCOLUM,L)=SWAP
260 INDEX(I,1)=IROW
    INDEX(I,2)=ICCOLUM
    PIVOT(I)=A(ICCOLUM,ICCOLUM)
    PIVOTI=PIVOT(I)
    IF(ABS(PIVOCI)-DEL)903,320,320
903 KC=2
320 DETERM=DETERM#PIVOTI
    A(ICCOLUM,ICCOLUM)=1.0
    DO 350 L=1,N
350 A(ICCOLUM,L)=A(ICCOLUM,L)/PIVOTI
    IF(M) 380, 380, 360
360 CC 370 L=1,M
370 B(ICCOLUM,L)=B(ICCOLUM,L)/PIVOTI
380 DO 550 LI=1,N
    IF(LI-ICCOLUM) 400, 550, 400
400 F=A(LI,ICCOLUM)

```

```

MATIN030
MATIN031
MATIN032
MATIN033
MATIN034
MATIN035
MATIN036
MATIN037
MATIN038
MATIN039
MATIN040
MATIN041
MATIN042
MATIN043
MATIN044
MATIN045
MATIN046
MATIN047
MATIN048
MATIN049
MATIN050
MATIN051
MATIN052

```

```

A(L1,ICOLUMN)=0.0
DC 450 L=1,N
450 A(L1,L)=A(L1,L)-A(ICOLUMN,L)*T
IF(M) 550, 550, 460
460 DC 500 L=1,M
500 B(L1,L)=B(L1,L)-B(ICOLUMN,L)*T
550 CONTINUE
DO 710 I=1,N
L=N+1-I
IF (INDEX(L,1)-INDEX(L,2)) 630, 710, 630
630 JROW=INDEX(L,1)
JCOLUMN=INDEX(L,2)
DC 705 K=1,N
SWAP=A(K,JROW)
A(K,JROW)=A(K,JCOLUMN)
A(K,JCOLUMN)=SWAP
705 CONTINUE
710 CCNTINUE
DO 900 J=1,N
IF(PIVOT(J)-1)900,900,901
900 CCNTINUE
740 RETURN
901 DETERM=0.
KC=3
GO TO 74C
END
MATIN053
MATIN054
MATIN055
MATIN056
MATIN057
MATIN058
MATIN059
MATIN060
MATIN061
MATIN062
MATIN063
MATIN064
MATIN065
MATIN066
MATIN067
MATIN068
MATIN069
MATIN070
MATIN071
MATIN072
MATIN073
MATIN074
MATIN075
MATIN076
MATIN077
MATIN078

```

```

SUBROUTINE INVERT(A,C,K)
IMPLICIT REAL*8 (A-H,C-Z)
DIMENSION A(12,12),E(12,1),PIVOT(12),IPIVOT(12),INDEX(12,2),
$C(12,12)
DO 1 I=1,K
DC 1 J=1,K
1 C(I,J)=A(I,J)
CALL MATINC(C,K,E,O,DETERM,KC,PIVOT,IPIVOT,INDEX)
RETURN
END

```

```

SUBROUTINE INVET2(A,C,N)
IMPLICIT REAL*8 (A-H,O-Z)
DIMENSION A(3,3),E(3,1),PIVOT(3),IPIVOT(3),INDEX(3,2),C(3,3)
DO 1 I=1,N
DC 1 J=1,N
1 C(I,J)=A(I,J)
CALL MATINC(C,N,E,O,DETERM,KC,PIVOT,IPIVOT,INDEX)
RETURN
END

```

```

SUBROUTINE INVET3(A,C,P)
IMPLICIT REAL*8 (A-H,O-Z)
DIMENSION A(13,13),E(13,1),PIVOT(13),IPIVOT(13),INDEX(13,2),
$C(13,13)
INTEGER P
DO 1 I=1,P
DC 1 J=1,P
1 C(I,J)=A(I,J)
CALL MATINC(C,P,E,O,DETERM,KC,PIVOT,IPIVOT,INDEX)
RETURN
END

```

```
SUBROUTINE TRANS(A,B,N1,N2)
DOUBLE PRECISION A(N1,N2),B(N2,N1)
DO 1 I=1,N1
DO 1 J=1,N2
1 B(J,I)=A(I,J)
RETURN
END

SUBROUTINE MULT(A,B,C,N1,N2,N3,N4)
DOUBLE PRECISION A(N1,N2),B(N3,N4),C(N1,N4)
DOUBLE PRECISION SUM
IF(N2.NE.N3) PRINT 2
2 FORMAT(3X,' MATRICES DO NOT MATCH IN MULT')
DO 1 I=1,N1
DO 1 J=1,N4
SUM=0.DO
DO 3 K=1,N3
3 SUM=SUM+A(I,K)*B(K,J)
1 C(I,J)=SUM
RETURN
END
```

```

SUBROUTINE FUNC(A,P,F,FB,FP)
IMPLICIT REAL*8(A-H,O-Z)
INTEGER PD
DIMENSION A(3,1),P(13,1),F(12,1),FB(12,3),FP(12,13)
DIMENSION Z(13),ZPRIM(13)
COMMON K,N,PD
A(1,1)=VOLUME RATIO, A(1,1) I=2,N VIRIAL COEFF
P=MEASURED PRESSURE, P=K+1
F=CONSTRAIN EQUATION, FB=PARTIALF/PARTIALB,FP=PARTIALF/PARTIALP
NN=NUMBER OF VIRIAL CCEFF TO BE EVALUATED
KI=K
ZERO=0.00
CNE=1.00
TWO=2.00
THREE=3.00
DC 1 I=1,PD
Z(I)=CNE
ZPRIM(I)=ZERO
NN=N
DC 1 J=2,NN
K=J
Z(I)=Z(I)+A(M,I)*P(I,1)**(J-1)
1 ZPRIM(I)=ZPRIM(I)+(J-1)*A(M,1)*P(I,1)**(J-2)
DC 2 I=1,K
DC 2 J=1,PD
2 FP(I,J)=ZERO
DC 3 L=1,K
J=L
ALPH=L.0803D-07
VRPRIM=(ONE+(ALPH*P(J+1,1)))/(CNE+(ALPH*P(J,1)))
VCLRAT=A(1,1)*VRPRIM
F(L,1)=P(J,1)*Z(J+1)-VCLRAT*P(J+1,1)*Z(J)
FP(L,J)=Z(J+1)-VCLRAT*P(J+1,1)*ZPRIM(J)+VCLRAT*P(J+1,1)*

```

C  
C  
C  
C

```
$(ALPH/(CNE+ALPH*P(J,1)))*Z(J)
FP(L,J+1)=P(J,1)*ZPRIM(J+1)-VCLRAT*Z(J)-((A(1,1))*P(J+1,1)*ALPH)/
$(CNE+ALPH*P(J,1))*Z(J)
FB(L,1)=-VRPRIM*P(J+1,1)*Z(J)
DC 3 I=2,NN
M=1
3 FB(L,M)=P(J,1)*P(J+1,1)**(I-1)-VCLRAT*P(J+1,1)*P(J,1)**(I-1)
RETURN
END
```



```

SUBROUTINE READ(X,Z,R,K,N,P,ITER)
  IMPLICIT REAL*8(A-H,O-Z)
  DIMENSION ZM(13,1)
  DIMENSION X(3,1),Z(13,1),R(13,13)
  INTEGER P
  THIS IS THE SUBPRCGRAM FOR READING THE INPUT DATA
  K=NUMBER OF EXPANSION OR NUMBER OF CONSTRAIN EQUATION
  N=NUMBER OF VIRIAL COEFF TO BE EVALUATED
  P=NUMBER OF MEASURED PRESSURE POINTS
  ITER= NUMBER OF ITERATION NEEDED
  X(1,1)= VOLUME RATIO, X(I,1)=ESTIMATED VIRIAL COEFF,(I=2,N)
  Z(I,1)=MEASURED PRESSURE.(I=1,P)
  R=WEIGHT FACTOR
  READ 4,K,N,P,ITER
  4 FORMAT(4I5)
  PRINT 12,K,N,P,ITER
  12 FORMAT (//4I5//)
  1 READ 1,(Z(I,1),I=1,P)
  1 FORMAT(F20.10)
  PRINT 13,(Z(I,1),I=1,P)
  13 FORMAT(F20.10)
  DC 6 I=1,P
  6 Z(I,1)=Z(I,1)/14.69600
  PRINT 15,(Z(I,1),I=1,P)
  15 FORMAT(F30.10)
  READ 2,(X(I,1),I=1,N)
  2 FORMAT(3E10.5)
  PRINT 14,(X(I,1),I=1,N)
  14 FORMAT(//3F30.10//)
  DC 7 I=1,P
  7 ZM(I,1)=3.000+Z(I,1)
  DC 3 I=1,P
  DC 3 J=1,P

```

```
R(I,J)=0.00  
3 R(I,I)=Z*(I,I)**2  
RETURN  
END
```

```
SUBROUTINE SKIP  
WRITE (6,I)  
1 FORMAT(IH)  
RETURN  
END
```

**APPENDIX E**

**ORIGINAL DATA**

TABLE E-1  
ORIGINAL DATA

HELIUM  
4/2/73

ISOTHERM 200°C

RUN 1

EXPANSION NUMBER	DWG WEIGHTS	DWG TEMP(°C)	CELL TEMP OHMS	ROOM TEMP (°C)	BARO mmHg	TIME
0	ABCDEFGLMOPSW34	25.0	45.3111	26.0	746.7	10:30
1	ABCDEOQRSTWX4	25.0	45.3108	25.9	746.6	11:40
2	ABCLOQRTUWX3	25.0	45.3112	26.0	746.0	12:40
3	ABLQVW123	25.0	45.3112	26.0	745.7	13:50
4	ALMPTWX1234	25.0	45.3111	26.0	745.5	14:30
5	ANST124	25.0	45.3113	25.9	745.0	15:20
6	LNOQSU34	25.0	45.3110	26.0	744.6	16:00
7	LPSX34	25.0	45.3112	26.0	744.6	16:50
8	MOPSTV123	25.0	45.3111	26.0	744.6	18:00
9	MQST123	25.0	45.3112	26.0	744.6	19:00
10	OQSUVX1234	25.0	45.3112	26.0	744.6	20:00

TABLE E-1 (CONTINUED)

## ORIGINAL DATA

HELIUM

4/8/73

RUN 2

ISOTHERM 200°C

EXPANSION NUMBER	DWG WEIGHTS	DWG TEMP (°C)	CELL TEMP OHMS	ROOM TEMP (°C)	BARO mmHg	TIME
0	ABCDEFHGOQTUVX34	25.0	45.3112	26.0	751.7	10:30
1	ABCDELORQWX124	25.0	45.3112	26.0	751.1	11:30
2	ABLMPQSTWX3	25.0	45.3110	26.0	750.5	12:40
3	ABLMPQSTUW12	25.0	45.3112	26.0	749.6	13:20
4	ALMNRQVWX123	25.0	45.3111	26.0	749.6	14:10
5	AMOQRTU123	25.0	45.3110	26.0	749.3	15:00
6	LMNR TX	25.0	45.3112	26.0	748.1	15:50
7	LOQTWX14	25.0	45.3113	26.0	747.9	16:40
8	MNSUVX123	25.0	45.3113	26.0	747.9	18:00
9	NPSUVX24	25.0	45.3113	26.0	747.8	18:50
10	OPTUW14	25.0	45.3113	26.0	747.7	19:30

TABLE E-1 (CONTINUED)

ORIGINAL DATA

HELIUM

4/12/73

ISOTHERM 250°C

RUN 3

EXPANSION NUMBER	DWG WEIGHTS	DWG TEMP(°C)	CELL TEMP OHMS	ROOM TEMP (°C)	BARO mmHg	TIME
0	ABCDEFGOPQSTW3	25.0	50.0646	26.0	743.4	11:00
1	ABCDERSIV124	25.0	50.0648	26.0	743.3	12:30
2	ABCLQTUVX3	25.0	50.0646	26.0	743.2	13:20
3	ABMNPSIVX124	25.0	50.0645	26.0	742.4	14:30
4	ALNSTUW124	24.8	50.0645	25.8	742.2	15:20
5	AOPQSTVWX	24.8	50.0647	25.8	742.0	16:00
6	LNOSUW14	24.8	50.0649	25.8	741.6	16:50
7	LQRTUI2	24.8	50.0648	25.8	741.4	18:30
8	NOPTUWX12	24.8	50.0646	25.8	741.5	19:20
9	MQTI	24.8	50.0646	25.8	741.2	20:00
10	OQSL34	24.8	50.0645	25.8	741.3	21:00

TABLE E-1 (CONTINUED)

ORIGINAL DATA

HELIUM

4/14/73

RUN 4

ISOTHERM 250°C

EXPANSION NUMBER	DWG WEIGHTS	DWG TEMP (°C)	CELL TEMP OHMS	ROOM TEMP (°C)	BARO mmHg	TIME
0	ABCDEFGHLMNPQTUV4	25.0	50.0648	26.0	742.5	09:30
1	ABCDEFNQRWL3	25.0	50.0648	26.0	742.1	10:20
2	ABCDMNS1	24.5	50.0642	25.5	741.7	11:20
3	ABCPRSTVW234	24.5	50.0643	25.5	741.4	12:10
4	ABOPTWX3	24.8	50.0643	25.8	741.7	13:10
5	AMNPQRTVWL2	24.8	50.0645	25.8	741.7	14:00
6	AQSUX34	25.0	50.0646	26.0	742.4	14:50
7	LNUX13	25.0	50.0646	26.0	742.5	15:50
8	MNPSTUV	25.0	50.0646	26.0	743.3	16:40
9	MOUW1	25.0	50.0646	26.0	742.9	17:30
10	OPQSTX34	25.0	50.0646	26.0	743.4	18:30

TABLE E-1 (CONTINUED)

## ORIGINAL DATA

FLUOROFORM

5/18/73

RUN 5

ISOTHERM 200°C

EXPANSION NUMBER	DWG WEIGHTS	DWG TEMP (°C)	CELL TEMP OHMS	ROOM TEMP (°C)	BARO mmHg	TIME
0	ABCDEFGHIINOQRUVX124	24.0	45.3112	25.0	738.0	14:35
1	ABCDEFLNOSUW124	24.0	45.3109	25.0	737.3	15:55
2	ABCDLMNRSTUWX12	24.0	45.3109	25.0	737.1	16:40
3	ABCLPUV13	24.0	45.3113	25.0	736.6	17:50
4	ABLQSTUX14	24.0	45.3111	25.0	736.5	19:00
5	ALMPQRTW124	24.0	45.3107	25.0	736.2	19:40
6	AMPTUV4	24.0	45.3108	25.0	736.2	20:10
7	INOPQW124	24.0	45.3109	25.0	736.0	21:00
8	LPQRUW4	24.0	45.3110	25.0	735.6	21:40
9	NOPQRUWX34	24.0	45.3110	25.0	735.2	22:20
10	MPX2	24.0	45.3110	25.0	735.2	23:00
11	OQRTUVX3	24.0	45.3111	25.0	735.5	23:40
12	PQTU3	24.0	45.3111	25.0	735.9	00:30



TABLE E-1 (CONTINUED)

ORIGINAL DATA

FLUOROFORM

6/16/73

ISOTHERM 250°C

RUN 6

EXPANSION NUMBER	DWG WEIGHTS	DWG TEMP (°C)	CELL TEMP OHMS	ROOM TEMP (°C)	BARO mmHg	TIME
0	ABCDEFGHIILPQRTUVX2	24.2	50.0644	25.0	740.1	09:15
1	ABCDEFILMOPQRUV23	24.2	50.0645	25.0	739.4	10:25
2	ABC DLMNQRUX4	24.3	50.0645	25.1	739.5	11:20
3	ABCLQTUWX	24.3	50.0646	25.0	739.1	12:25
4	ABLUVX12	24.2	50.0646	25.0	738.8	13:30
5	ALMPSTW4	24.2	50.0646	25.1	738.1	14:30
6	ANQSUV14	24.2	50.0646	25.2	737.9	15:20
7	LMOPUX	24.2	50.0646	25.2	737.6	16:25
8	LPQTUV34	24.2	50.0646	25.0	737.2	17:30
9	MOPQSUX13	24.1	50.0645	25.0	736.6	18:20
10	MQRUX1	24.1	50.0645	25.0	736.6	19:10
11	OQRUVX134	24.1	50.0646	25.0	736.1	20:00
12	PQUWX123	24.1	50.0646	25.1	735.5	21:00

TABLE E-1 (CONTINUED)

ORIGINAL DATA  
FLUOROFORM

ISOTHERM 250°C

6/17/73

RUN 7

EXPANSION NUMBER	DWG WEIGHTS	DWG TEMP (°C)	CELL TEMP OHMS	ROOM TEMP (°C)	BARO mmHg	TIME
0	ABCDEFGHIJLQRTX13	24.3	50.0646	25.1	741.3	10:00
1	ABCDEFGLPQTUWX134	24.3	50.0646	25.1	741.5	11:00
2	ABCDEMNRWL23	24.2	50.0646	25.1	741.6	12:00
3	ABCLMOPQWX13	24.2	50.0647	25.0	742.0	13:00
4	ABLMPSTUWX4	24.2	50.0646	25.0	741.8	14:10
5	ALMNP TWX4	24.3	50.0646	25.1	741.3	15:00
6	AMOPQWL34	24.3	50.0645	25.1	741.4	16:00
7	LMNPX134	24.2	50.0646	25.0	741.1	17:40
8	LOQRTUV124	24.1	50.0646	25.0	740.9	18:40
9	MNQS UWX124	24.1	50.0646	25.0	740.8	19:30
10	MPQTUV124	24.2	50.0646	25.0	740.6	20:20
11	OPQ2	24.2	50.0646	25.0	740.2	21:10
12	PQRWX12	24.2	50.0646	25.0	740.0	22:00

TABLE E-1 (CONTINUED)

ORIGINAL DATA

FLUOROFORM

6/23/73

ISOTHERM 200°C

RUN 8

EXPANSION NUMBER	DWG WEIGHTS	DWG TEMP(°C)	CELL TEMP OHMS	ROOM TEMP (°C)	BARO mmHG	TIME
0	ABCDEFGHIIMPQRTW	24.0	45.3112	25.0	748.1	09:20
1	BCDEFGOQRTWX3	24.0	45.3112	25.0	747.7	10:20
2	ABCDEOPQST23	24.0	45.3113	25.1	747.0	11:30
3	ABCLMQSTX4	24.0	45.3112	25.1	747.1	12:20
4	ABLOPQ1	24.2	45.3113	25.1	746.6	13:30
5	ALMOPQRUX	24.2	45.3113	25.0	746.3	14:30
6	AMQQTUW13	24.2	45.3113	25.0	745.7	15:20
7	LMNQW3	24.2	45.3112	25.0	744.9	16:30
8	LOQTUW12	24.2	45.3112	25.0	744.6	17:30
9	MNSTUWX24	24.2	45.3112	25.0	744.1	18:30
10	MPSTUW12	24.2	45.3112	25.0	744.2	19:20
11	OPSWX124	24.2	45.3112	25.0	743.6	20:00
12	PQSTX14	24.2	45.3112	25.0	743.5	20:50

TABLE E-1 (CONTINUED)  
 ORIGINAL DATA  
 FLUOROFORM  
 6/28/73

RUN 9

ISOTHERM 300°C

EXPANSION NUMBER	DWG WEIGHTS	DWG TEMP (°C)	CELL TEMP OHMS	ROOM TEMP (°C)	BARO mmHG	TIME
0	ABCDEFGHIJKPQUVX3	24.0	54.7432	25.2	742.1	09:50
1	ABCDEFGHIJMNWX123	24.0	54.7432	25.2	741.6	11:00
2	ABCDEFGHIJQRUVX12	24.2	54.7431	25.3	742.1	11:50
3	ABCDQUV3	24.2	54.7430	25.3	741.6	13:00
4	ABLMOPTU12	24.2	54.7430	25.3	741.2	13:50
5	ABSTUW	24.2	54.7432	25.2	741.2	14:50
6	AMNST3	24.0	54.7432	25.2	740.4	15:40
7	LMNPQSUX3	24.0	54.7432	25.2	740.7	16:40
8	LOPQUX13	24.0	54.7432	25.2	740.4	18:00
9	MNPWL	24.0	54.7432	25.2	740.7	19:00
10	MPQRUI3	24.2	54.7430	25.2	740.6	19:50
11	OPQTUVX2	24.2	54.7430	25.2	741.2	20:40
12	PQRTUWX124	24.2	54.7431	25.2	741.5	21:40

TABLE E-1 (CONTINUED)  
 ORIGINAL DATA  
 FLUOROFORM  
 6/29/73

ISOTHERM 300°C

RUN 10

EXPANSION NUMBER	DWG WEIGHTS	DWG TEMP (°C)	CELL TEMP OHMS	ROOM TEMP (°C)	BARO mmHg	TIME
0	ABCDEFGHIJLOFQTUW12	24.0	54.7431	25.2	741.0	08:50
1	ABCDEFGHILOQW12	24.0	54.7431	25.2	741.6	09:50
2	ABCDEMNRUWX4	24.0	54.7431	25.2	741.4	10:40
3	ABCLMOPQTUWX124	24.0	54.7430	25.0	741.2	11:40
4	ABLMPUX13	24.0	54.7430	25.0	740.9	12:30
5	ALMNRUX14	24.0	54.7432	25.0	740.8	13:20
6	AMOPSW	24.2	54.7432	25.0	740.6	14:20
7	LMNRUWX134	24.2	54.7435	25.2	740.3	15:00
8	LOQRT4	24.2	54.7434	25.2	740.0	16:00
9	MNQSX12	24.2	54.7434	25.4	740.0	17:10
10	MPQTUW3	24.2	54.7432	25.4	739.6	18:00
11	OPSTUVX24	24.2	54.7431	25.4	739.2	18:50
12	PQRWX12	24.2	54.7430	25.3	739.6	19:40

TABLE E-1 (CONTINUED)  
 ORIGINAL DATA  
 FLUOROFORM  
 7/6/73

ISOTHERM 350°C

RUN 11

EXPANSION NUMBER	DWG WEIGHTS	DWG TEMP (°C)	CELL TEMP OHMS	ROOM TEMP (°C)	BARO mmHg	TIME
0	ABCDEFGLMNT3	24.2	59.3471	25.4	746.9	09:30
1	ABCDEFMQRTUX124	24.2	59.3470	25.4	746.5	10:20
2	ABCDLQW134	24.2	59.3470	25.6	746.5	11:20
3	ABCMSW3	24.2	59.3471	25.6	746.2	12:00
4	ABMPQ123	24.2	59.3469	25.6	745.6	13:10
5	ALPQRTX3	24.2	59.3469	25.6	745.2	14:00
6	AOSWX134	24.2	59.3469	25.4	745.7	14:50
7	LMPST12	24.2	59.3470	25.4	745.3	15:50
8	LSTUX4	24.2	59.3470	25.4	745.0	16:40
9	MOQR134	24.2	59.3470	25.4	745.3	17:40
10	MUSW2	24.2	59.3471	25.4	745.8	18:30
11	OQUW24	24.2	59.3472	25.4	746.0	19:20
12	PTUWX34	24.2	59.3471	25.4	746.5	20:00

TABLE E-1 (CONTINUED)  
 ORIGINAL DATA  
 FLUOROFORM  
 7/7/73

RUN 12

ISOTHERM 350°C

EXPANSION NUMBER	DWG WEIGHTS	DWG TEMP (°C)	CELL TEMP OHMS	ROOM TEMP (°C)	BARO mmHg	TIME
0	ABCDEFGHIJQRUWX23	24.0	59.3471	25.4	745.1	07:30
1	ABCDEFMLMUL2	24.0	59.3471	25.4	745.3	08:20
2	ABCDDLMOQRT3	24.0	59.3470	25.5	744.9	09:10
3	ABCMNQRT3	24.0	59.3470	25.5	744.1	10:00
4	ABMNQSTUW123	24.2	59.3470	25.5	744.1	11:00
5	ALMSTW4	24.2	59.3469	25.5	744.7	11:50
6	AOPQRTUW34	24.2	59.3470	25.5	745.3	12:40
7	LMOQTU3	24.2	59.3471	25.5	746.0	13:30
8	LPSWX3	24.2	59.3470	25.5	746.2	14:30
9	MOPQWX13	24.2	59.3470	25.5	746.5	15:20
10	MQSTX3	24.2	59.3470	25.5	746.9	16:10
11	OQSTUV14	24.2	59.3470	25.5	747.1	17:00

TABLE E-1 (CONTINUED)

ORIGINAL DATA

HELIUM

7/15/73

ISOTHERM 300°C

RUN 13

EXPANSION NUMBER	DWG WEIGHTS	DWG TEMP (°C)	CELL TEMP OHMS	ROOM TEMP (°C)	BARO mmHg	TIME
0	ABCDEFGHIJKLMNQRSTUWX 124	24.0	54.7432	25.0	746.0	09:15
1	ABCDEFGHIMPQRTUV1	24.0	54.7434	25.0	745.6	10:15
2	ABCDMNQST134	24.0	54.7432	25.2	745.3	11:10
3	ABCOSTUV24	24.0	54.7432	25.2	745.1	12:00
4	ABOPQSTU124	24.0	54.7431	25.2	745.0	13:05
5	ALQTW123	24.0	54.7432	25.2	744.7	14:00
6	APTU	24.0	54.7432	25.2	744.8	14:50
7	LMQUW34	24.0	54.7431	25.2	744.3	15:40
8	MNPQSTX2	24.0	54.7432	25.2	743.8	16:15
9	MOSTWX34	24.0	54.7435	25.2	743.6	17:00
10	OPQRTW134	24.0	54.7433	25.2	743.2	17:50
11	OSX4	24.0	54.7432	25.2	743.2	18:40



TABLE E-1 (CONTINUED)

## ORIGINAL DATA

HELIUM

7/17/73

RUN 14

ISOTHERM 300°C

EXPANSION NUMBER	DWG WEIGHTS	DWG TEMP (°C)	CELL TEMP OHMS	ROOM TEMP (°C)	BARO mmHg	TIME
0	ABCDEFGMOPQRUVX34	24.0	54.7432	24.8	748.1	09:30
1	ABCDEMTWX13	24.0	54.7432	24.8	747.8	10:30
2	ABCLOPSUV12	24.0	54.7434	24.8	747.6	11:20
3	AML PQWX3	24.2	54.7434	25.0	747.4	12:15
4	ALMOX	24.2	54.7430	25.0	747.0	13:00
5	AMPWX2	24.2	54.7432	25.0	746.4	14:00
6	LMOPSWX4	24.2	54.7430	24.8	746.2	14:50
7	LPQSUV4	24.2	54.7432	25.2	746.1	15:35
8	MOPQSTWX4	24.2	54.7434	25.2	746.6	16:20
9	MQRTX123	24.2	54.7432	25.2	746.6	17:10
10	OQRTX14	24.2	54.7430	25.2	747.4	18:00

TABLE E-1 (CONTINUED)

ORIGINAL DATA

HELIUM

ISOTHERM 350 °C

7/21/73

RUN 15

EXPANSION NUMBER	DWG WEIGHTS	DWG TEMP (°C)	CELL TEMP OHMS	ROOM TEMP (°C)	BARO mmHg	TIME
0	ABCDEFGHIJKLMNQSUVX13	24.0	59.3470	25.0	744.8	09:00
1	ABCDEFGHILOP23	24.0	59.3472	25.2	744.9	10:10
2	ABCDLOPQRSTUWX123	24.0	59.3472	25.2	745.1	11:00
3	ABCMOUX4	24.2	59.3470	25.2	745.3	12:00
4	ABMOR	24.2	59.3468	25.2	744.5	12:50
5	ALOQU24	24.2	59.3467	25.2	744.4	13:40
6	AOQTW13	24.2	59.3468	25.0	744.3	14:40
7	IMPQUW1	24.2	59.3468	25.0	744.1	15:20
8	LQWX134	24.2	59.3470	25.0	743.5	16:00
9	MOQRUX1	24.2	59.3470	25.0	744.2	16:40
10	MST3	24.2	59.3470	25.0	744.3	17:30
11	OQUV4	24.2	59.3471	25.2	744.4	18:20

TABLE E-1 (CONTINUED)

## ORIGINAL DATA

HELIUM

7/22/73

ISOTHERM 350°C

RUN 16

EXPANSION NUMBER	DWG WEIGHTS	DWG TEMP (°C)	CELL TEMP OHMS	ROOM TEMP (°C)	BARO mmHg	TIME
0	ABCDEFGHIQSTL3	24.0	59.3472	25.2	747.3	09:50
1	ABCDEFMNQSTUVX3	24.0	59.3472	25.2	747.5	10:40
2	ABCDLQRL	24.2	59.3470	25.2	747.0	11:30
3	ABCOPQRTU3	24.2	59.3472	25.4	746.9	12:20
4	ABMQRT4	24.2	59.3473	25.4	746.6	13:20
5	ALPSTUV4	24.2	59.3470	25.4	745.9	14:10
6	APQSTUW12	24.2	59.3470	25.4	745.4	15:00
7	LMQRTW2	24.2	59.3470	25.4	745.1	16:00
8	LUI23	24.2	59.3468	25.4	745.5	16:50
9	MOQTUWX12	24.2	59.3468	25.4	745.5	17:40
10	MT34	24.2	59.3468	25.2	746.5	18:30
11	OSTWX12	24.2	59.3470	25.2	746.7	19:10

TABLE E-2  
DEAD WEIGHT GAUGE CONSTANTS  
AND WEIGHT CALIBRATIONS

APPARENT MASS VS BRASS POUNDS  
GAUGE NUMBER

DESIGNATION	1	2	3 AND 4
TARE	0.104056	0.0260145	0.78107
A	1.30074	1.30075	26.03608
B	1.30074	1.30074	26.03606
C	1.30071	1.30076	26.03600
D	1.30072	1.30076	26.03594
E	1.30073	1.30075	26.03602
F	-	-	26.03612
G	0.650368	0.520298	26.03596
H	0.130071	0.520298	26.03599
I	0.130073	0.260147	26.03577
J	0.130070	0.130077	26.03622
K	0.130076	0.0520309	26.03588
L	0.130073	0.0520306	13.01828
M	0.0650359	0.0260150	5.20698
N	0.0260148	0.0130068	5.20709
O	0.0260143	0.0065039	2.60359
P	0.0130075	-	1.30182
Q	0.0065036	-	0.52074
R	-	-	0.52072
S	-	-	0.26038
T	-	-	0.13017
U	-	-	0.05210
V	-	-	0.05209
W	-	-	0.02605
X	-	-	0.01302
1	0.0026015	0.0026015	0.0052027
2	0.0026012	0.0026015	0.0051989
3	0.0013005	0.0013007	0.0026012
4	0.0009509	0.0006506	0.0013009

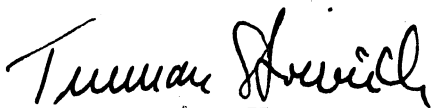
The undersigned, appointed by the Dean of the Graduate Faculty, have examined a thesis entitled

PVT MEASUREMENTS ON FLUOROFORM: SECOND AND THIRD  
VIRIAL COEFFICIENTS FROM 200°C TO 350°C AND  
COMPRESSIBILITY FACTORS TO 150 ATMOSPHERES

presented by Wen-Shou Liou

a candidate for the degree of Doctor of Philosophy

and hereby certify that in their opinion it is worthy of acceptance.



Truman S. Storvick  
Professor  
Chemical Engineering  
Department



Richard H. Luecke  
Associate Professor  
Chemical Engineering  
Department



Keum H. Lee  
Associate Professor  
Physics Department

Digitization Information Page

Local identifier Liou1974

Source information

Format Book

Content type Text

Source ID Gift copy from department; not added to MU collection.

Notes

Capture information

Date captured July 2023

Scanner manufacturer Fujitsu

Scanner model fi-7460

Scanning system software ScandAll Pro v. 2.1.5 Premium

Optical resolution 600 dpi

Color settings 8 bit grayscale

File types tiff

Notes

Derivatives - Access copy

Compression Tiff: LZW compression

Editing software Adobe Photoshop

Resolution 600 dpi

Color grayscale

File types pdf created from tiffs

Notes Images cropped, straightened, brightened